CHAPTER - 1

DIFFRACTION OF WAVES

[1]HIGH FREQUENCY SCATTERING DUE TO A PAIR OF TIME-HARMONIC ANTIPLANE FORCES ON THE FACES OF A FINITE INTERFACE CRACK BETWEEN DISSIMILAR ANISOTROPIC MATERIALS

1. INTRODUCTION

The extensive use of composite materials in modern technology has created interest among the scientists for carrying on considerable research work in the modeling, testing and analysis of laminated media. The laminated composites which behave as anisotropic material may be weakened by interface flaws which can lead to serious degradation in load carrying capacity.

Neerhoff [1979], therefore, studied the diffraction of Love waves by a crack of finite width at the interface of a layered half-space. Kuo [1992] carried out numerical and analytical studies of transient response of an interfacial crack between two dissimilar orthotropic half-spaces. Kuo and Cheng [1991] studied the elastodynamic responses due to antiplane point impact loading on the faces of a semi-infinite crack lying at the interface of two dissimilar anisotropic elastic materials. The problem of diffraction of normally incident antiplane shear wave by a crack of finite width situated at the interface of two bonded dissimilar isotropic elastic half-spaces has been studied by Pal and Ghosh [1990].

In the present paper we are interested in finding the high-frequency solution of the diffraction of elastic waves by a Griffith crack of finite width excited by a pair of time-harmonic concentrated antiplane line loads situated at the centres of the cracked surfaces. The materials are assumed to possesss certain material symmetry and the crack plane is assumed to coincide with one of the planes

---

[1] **Published in the European Journal of Mechanics A/Solids, V18, 1013-1026, 1999.**

of material symmetry, so that the inplane and the antiplane motion are not coupled.

The high-frequency solution of the diffraction of elastic waves by a crack of finite size is interesting in view of the fact that the transient solution close to the wave front can be represented by an integral of the high-frequency component of the solution. The analysis of the paper is first based on the observation of several researchers, e.g., Achenbach and Kuo [1986], Ma and Hou [1989], Markenscoff and Ni [1984] that antiplane shear deformation in an anisotropic solid can be deduced from the corresponding deformations of an isotropic solid by a transformation of relevant co-ordinates and parameters. Based on this observation, analysis of the interface crack by line loads between two bonded dissimilar anisotropic elastic solids can first be converted to that of a crack between two dissimilar isotropic elastic materials. Later, following the method of Chang [1971], the problem has been formulated as an extended Wiener-Hopf equation. The Wiener-Hopf equation in brief can be found in the book of Achenbach [1973]. The asymptotic solutions for high-frequencies or for wave lengths short compared to the width of the crack have been derived. Expression for the dynamic stress intensity factor near the crack tips has been obtained and the results have been illustrated for different pairs of materials.

2. FORMULATION OF THE PROBLEM

Let (X,Y,Z) be rectangular Cartesian co-ordinates. The X-axis is taken along the interface, Y-axis vertically upwards into the medium and Z-axis is perpendicular to the plane of the paper. Let an open crack of finite width 2L be located at the interface of two bonded dissimilar anisotropic semi-infinite elastic solids lying parallel to X-axis. The anisotropic half-planes are characterized by the elastic moduli $(C_{ik})_j$; (i,k=4,5) and mass density $\bar{\rho}_j$. The subscript j (j=1,2) corresponds to the

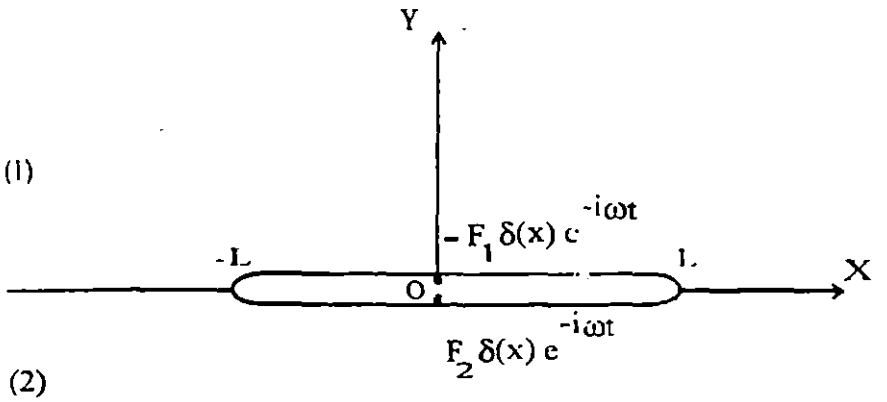

Fig.1. Geometry of the problem.

upper and lower semi-infinite media respectively.

A pair of concentrated time-harmonic antiplane shear forces in the Z-direction of magnitudes F_1 and F_2 act on the crack faces Y=0+ and Y=0- respectively at X=0 as shown in Fig.1. Thus the crack boundary conditions are

$$\sigma_{YZ}(X,Y,t) = \begin{cases} -F_1\delta(X)e^{-i\omega t}; & |X|<L, \quad Y=0+, \\ F_2\delta(X)e^{-i\omega t}; & |X|<L, \quad Y=0-, \end{cases} \tag{1}$$

$$\sigma^{(1)}_{YZ}(X,Y,t) = \sigma^{(2)}_{YZ}(X,Y,t) \quad \text{at } Y=0, \quad |X|>L \tag{2}$$

$$W_1(X,Y,t) = W_2(X,Y,t) \quad \text{at } Y=0, \quad |X|>L, \tag{3}$$

where ω is the circular frequency. Two dimensional antiplane wave motions of homogeneous anisotropic linearly elastic solids are governed by

$$(C_{55})_j \frac{\partial^2 W_j}{\partial X^2} + 2(C_{45})_j \frac{\partial^2 W_j}{\partial X \partial Y} + (C_{44})_j \frac{\partial^2 W_j}{\partial Y^2} = \bar{\rho}_j \frac{\partial^2 W_j}{\partial t^2} \qquad (j=1,2), \tag{4}$$

where W_j (X,Y,t) are the out-of-plane displacements.

The XY-plane has been assumed to coincide with one of the planes of material symmetry such that inplane and anti-plane motions are not coupled.

The relevant stress components are

$$\sigma^{(j)}_{XZ} = (C_{55})_j \frac{\partial W_j}{\partial X} + (C_{45})_j \frac{\partial W_j}{\partial Y}, \tag{5}$$

$$\sigma^{(j)}_{YZ} = (C_{45})_j \frac{\partial W_j}{\partial X} + (C_{44})_j \frac{\partial W_j}{\partial Y}. \tag{6}$$

Following Achenbach and Kuo [1986] and Kuo and Cheng [1991] we introduce a co-ordinate transformation

$$\left.\begin{aligned} x &= X - \frac{(C_{45})_j}{(C_{44})_j} Y, \\ y &= \frac{\mu_j}{(C_{44})_j} Y, \\ z &= Z, \end{aligned}\right\} \qquad (j=1,2) \tag{7}$$

where

$$\mu_j = \sqrt{(C_{44})_j (C_{55})_j - (C_{45})_j^2} \qquad (j = 1, 2). \tag{8}$$

Equation (7) and the chain rule of diffrentiation reduced (4) to the standard wave equation

$$\frac{\partial^2 W_j}{\partial x^2} + \frac{\partial^2 W_j}{\partial y^2} = s_j^2 \frac{\partial^2 W_j}{\partial t^2}, \tag{9}$$

where

$$s_j^2 = \frac{\rho_j}{\mu_j} \quad \text{and} \quad \rho_j = \frac{\bar{\rho}_j (C_{44})_j}{\mu_j}, \tag{10}$$

s_j is the slowness of shear waves. Without loss of generality we assume that

$$s_1 < s_2 . \tag{11}$$

Assume

$$W_j(x,y,t) = w_j(x,y) e^{-i\omega t}, \qquad j = 1,2, \tag{12}$$

so that $w_j(x,y)$ satisfy the following Helmholtz equations

$$\nabla^2 w_j(x,y) + k_j^2 w_j(x,y) = 0, \qquad j = 1,2, \tag{13}$$

with $\nabla^2 = \frac{\partial^2}{\partial x^2} + \frac{\partial^2}{\partial y^2}$ and $k_j = \omega s_j$, $j=1,2$.

It follows from equation (11) that $k_2 > k_1$.

It is easily verified from (4), (5) and (6) that the relevant displacement and the stress component in a physical anisotropic solid are related to those in the corresponding isotropic solid by

$$W_j(X,Y,t) = W_j(x,y,t), \tag{14}$$

$$\sigma_{XZ}^{(j)}(X,Y,t) = \frac{\mu_j}{(C_{44})_j} \sigma_{xz}^{(j)}(x,y,t) + \frac{(C_{45})_j}{(C_{44})_j} \sigma_{yz}^{(j)}(x,y,t), \tag{15}$$

$$\sigma_{YZ}^{(j)}(X,Y,t) = \sigma_{yz}^{(j)}(x,y,t). \tag{16}$$

Further writing

$$\sigma_{yz}^{(j)}(x,y,t) = \tau_{yz}^{(j)}(x,y) e^{-i\omega t}, \qquad j = 1,2, \tag{17}$$

under the changed co-ordinate system the boundary conditions (1), (2) and (3) reduce to

$$\tau_{yz}^{(1)}(x,y) = \mu_1 \frac{\partial w_1}{\partial y} = -F_1\delta(x); \qquad |x|<L, \quad y=0+, \tag{18}$$

$$\tau_{yz}^{(2)}(x,y) = \mu_2 \frac{\partial w_2}{\partial y} = F_2\delta(x); \qquad |x|<L, \quad y=0- \tag{19}$$

and

$$\mu_1 \frac{\partial w_1}{\partial y} = \mu_2 \frac{\partial w_2}{\partial y}, \qquad |x|>L, \quad y=0, \tag{20}$$

$$w_1(x,0+) = w_2(x,0-), \qquad |x|>L. \tag{21}$$

To obtain the solution to the wave equation (13), introduce the Fourier transform defined by

$$\bar{w}(\alpha,y) = \frac{1}{\sqrt{2\pi}} \int_{-\infty}^{\infty} w(x,y) e^{i\alpha x} dx. \tag{22}$$

The transformed wave equations are

$$\frac{d^2\bar{w}_1}{dy^2} - (\alpha^2 - k_1^2)\bar{w}_1(\alpha,y) = 0, \qquad y \geq 0, \tag{23}$$

$$\frac{d^2\bar{w}_2}{dy^2} - (\alpha^2 - k_2^2)\bar{w}_2(\alpha,y) = 0, \qquad y \leq 0. \tag{24}$$

The solutions of (23) and (24) which are bounded as $y \to \infty$ are

$$\bar{w}_1(\alpha,y) = A_1(\alpha) e^{-\gamma_1 y}; \qquad y \geq o, \tag{25}$$

$$\bar{w}_2(\alpha,y) = A_2(\alpha) e^{\gamma_2 y}; \qquad y < o, \tag{26}$$

where

$$\gamma_j = \begin{cases} \sqrt{\alpha^2 - k_j^2}; & |\alpha| > k_j, \\ -i\sqrt{k_j^2 - \alpha^2}; & |\alpha| < k_j. \end{cases} \tag{27}$$

Introduce, for a complex α

$$G_+(\alpha) = \frac{1}{\sqrt{2\pi}} \int_{L}^{\infty} \tau_{yz}^{(1)}(x,0) e^{i\alpha(x-L)} dx, \tag{28}$$

$$G_-(\alpha) = \frac{1}{\sqrt{2\pi}} \int_{-\infty}^{-L} \tau_{yz}^{(1)}(x,0) e^{i\alpha(x+L)} dx, \tag{29}$$

$$G_j(\alpha) = \frac{1}{\sqrt{2\pi}} \int_{-L}^{L} \tau_{yz}^{(j)}(x,0) e^{i\alpha x} dx. \tag{30}$$

The transformed stress at interface y=0 can therefore be written as

$$\bar{\tau}_{yz}^{(j)}(\alpha,0) = G_+(\alpha) e^{i\alpha L} + G_-(\alpha) e^{-i\alpha L} + G_j(\alpha). \tag{31}$$

Using the boundary conditions (18) and (19), we get

$$G_j(\alpha) = (-1)^j \frac{F_j}{\sqrt{2\pi}} \quad (j = 1,2). \tag{32}$$

Now

$$\bar{\tau}_{yz}^{(1)}(\alpha,0+) = \mu_1 \frac{\partial \bar{w}_1(\alpha,0+)}{\partial y} = -\mu_1 \gamma_1 A_1(\alpha), \tag{33}$$

$$\bar{\tau}_{yz}^{(2)}(\alpha,0-) = \mu_2 \frac{\partial \bar{w}_2(\alpha,0-)}{\partial y} = \mu_2 \gamma_2 A_2(\alpha). \tag{34}$$

Using (33) and (34), equation (31) can be written in the form

$$(-1)^j \mu_j \gamma_j A_j(\alpha) = G_+(\alpha) e^{i\alpha L} + G_-(\alpha) e^{-i\alpha L} + (-1)^j \frac{F_j}{\sqrt{2\pi}}.$$

Therefore

$$A_j(\alpha) = \frac{(-1)^j}{\mu_j \gamma_j} \left[G_+(\alpha) e^{i\alpha L} + G_-(\alpha) e^{-i\alpha L} + (-1)^j \frac{F_j}{\sqrt{2\pi}} \right]. \tag{35}$$

Now

$$\bar{w}_1(\alpha,0+) - \bar{w}_2(\alpha,0-) = \frac{1}{\sqrt{2\pi}} \int_{-L}^{L} \left\{ w_1(x,0+) - w_2(x,0-) \right\} e^{i\alpha x} dx = B(\alpha), \text{ say}$$

which is the measure of the displacement discontinuity across the crack surface. Therefore

$$B(\alpha) = A_1(\alpha) - A_2(\alpha). \tag{36}$$

Substituting the values of $A_j(\alpha)$ from (35) in equation (36) one finds an extended Wiener-Hopf equation namely

$$G_+(\alpha) e^{i\alpha L} + G_-(\alpha) e^{-i\alpha L} + B(\alpha) K(\alpha) = \frac{K(\alpha)}{\sqrt{2\pi}} \left\{ \frac{F_1}{\mu_1 \gamma_1} - \frac{F_2}{\mu_2 \gamma_2} \right\}, \tag{37}$$

where

$$K(\alpha) = \frac{\mu_1 \mu_2 \gamma_1 \gamma_2}{\mu_1 \gamma_1 + \mu_2 \gamma_2} = \frac{\mu_1 \mu_2 \sqrt{\alpha^2 - k_1^2}}{\mu_1 + \mu_2} R(\alpha) \tag{38}$$

and

$$R(\alpha) = \frac{(\mu_1+\mu_2)\sqrt{(\alpha_2-k_2^2)}}{\mu_1\sqrt{(\alpha_2-k_1^2)}+\mu_2\sqrt{(\alpha_2-k_2^2)}}. \qquad (39)$$

In order to obtain the high-frequency solution of the Wiener-Hopf equation given by (37) one assumes that the branch points $\alpha=k_1$ and $\alpha=k_2$ of $K(\alpha)$ possess a small imaginary part. Therefore k_1 and k_2 are replaced by k_1+ik_1' and k_2+ik_2' respectively where k_1' and k_2' are infinitesimally small positive quantities which would ultimately be made to tend to zero.

Now $K(\alpha)=K_+(\alpha)\,K_-(\alpha)$ where $K_+(\alpha)$ is analytic in the upper half-plane $\mathrm{Im}\alpha > -k_2'$ whereas $K_-(\alpha)$ is analytic in the lower half-plane $\mathrm{Im}\alpha < k_2'$ are given by (cf. Pal and Ghosh [1990]; Wickham [1980])

$$K_\pm(\alpha) = \sqrt{\frac{\mu_2(\alpha\pm k_1)}{1+m}}\exp\left[\frac{1}{\pi}\int_1^\gamma \frac{\tan^{-1}\left\{\dfrac{\sqrt{(t^2-1)}}{m\sqrt{(\gamma^2-t^2)}}\right\}}{t\pm\dfrac{\alpha}{k_1}}\,dt\right],$$

where $m=\dfrac{\mu_2}{\mu_1}$ and $\gamma=\dfrac{k_2}{k_1}$.

Since $\tau_{yz}(x,0)$ decreases exponentially as $x \to \pm\infty$, $G_+(\alpha)$ and $G_-(\alpha)$ have the common region of regularity as $K_+(\alpha)$ and $K_-(\alpha)$. It may be noted that $B(\alpha)$ is analytic in the whole of α-plane.

Now (37) can easily be expressed as two integral equations relating $G_+(\alpha)$, $G_-(\alpha)$ and $B(\alpha)$ as follows :

$$\frac{G_\pm(\alpha)}{K_\pm(\alpha)} + \frac{1}{2\pi i}\int_{C_\pm}\frac{G_\mp(s)e^{\mp 2isL}}{(s-\alpha)K_\pm(s)}ds - \frac{1}{2\pi i}\int_{C_\pm}\frac{e^{\mp isL}K_\mp(s)}{\sqrt{2\pi}(s-\alpha)}\left\{\frac{F_1}{\mu_1\gamma_1(s)}-\frac{F_2}{\mu_2\gamma_2(s)}\right\}ds$$

$$= -B(\alpha)K_\mp(\alpha)e^{\mp i\alpha L} - \frac{1}{2\pi i}\int_{C_\mp}\frac{G_\mp(s)e^{\mp 2isL}}{(s-\alpha)K_\pm(s)}ds + \frac{1}{2\pi i}\int_{C_\mp}\frac{e^{\mp isL}K_\mp(s)}{\sqrt{2\pi}(s-\alpha)}\left\{\frac{F_1}{\mu_1\gamma_1(s)}-\frac{F_2}{\mu_2\gamma_2(s)}\right\}ds, \qquad (40)$$

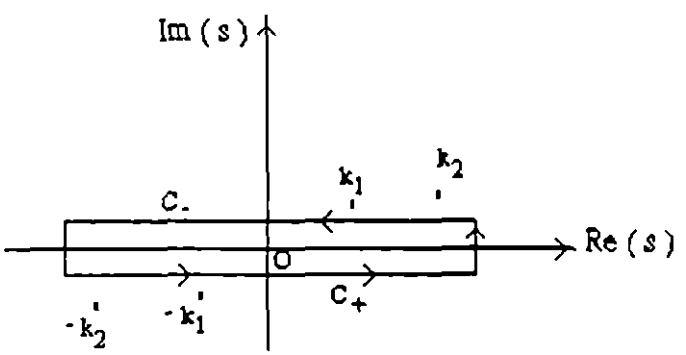

Fig.2. Path of integration in the complex s-plane.

where C_+ and C_- are the straight contours situated within the common region of regularity of $G_+(s)$, $G_-(s)$, $K_+(s)$ and $K_-(s)$ as shown in Fig.2.

In the first equation of (40) (i.e. the equation involving upper subscripts), the left-hand side is analytic in the upperhalf plane whereas the right-hand side is analytic in the lowerhalf plane and both of them are equal in the common region of analyticity of these two functions. So by analytic continuation, both sides of the equation are analytic in the whole of the s-plane. Now, since

$$\tau_{yz} = O(|x \mp L|^{-1/2}) \qquad \text{as} \quad x \to \pm L$$

so $$G_+(\alpha) = O(\alpha^{-1/2}) \qquad \text{as} \quad |\alpha| \to \infty, \quad \mathrm{Im}\alpha > 0$$

and also $$K_\pm(\alpha) = O(\alpha^{1/2}) \qquad \text{as} \quad |\alpha| \to \infty, \quad \mathrm{Im}\alpha \neq 0.$$

So it follows that

$$\frac{G_+(\alpha)}{K_+(\alpha)} = O(\alpha^{-1}) \qquad \text{as} \quad |\alpha| \to \infty, \quad \mathrm{Im}\alpha > 0.$$

Presumably one has $w_1(x,0+) - w_2(x,0-) = O(|x \mp L|^{1/2})$ as $x \to \pm L$.

Then it follows by standard Abelian asymptotics (cf. Noble [1958]; p.36) that

$$B(\alpha) = e^{i\alpha L} O(\alpha^{-3/2}) + e^{-i\alpha L} O(\alpha^{-3/2}) \quad \text{as} |\alpha| \to \infty.$$

Consequently one has

$$B(\alpha) K_-(\alpha) e^{-i\alpha L} = O(\alpha^{-1}) \qquad \text{as} \quad |\alpha| \to \infty, \quad \mathrm{Im}\alpha < 0.$$

Thus both sides of the first equation of (40) are $O(\alpha^{-1})$ as $|\alpha| \to \infty$ in the respective half-planes.

Therefore by Liouville's Theorem, both sides of the first equation of (40) are equal to zero. The second equation of (40) (i.e. the equation involving lower subscripts) can be treated similarly. Therefore from (40) one obtains the system of integral equations given by

$$\frac{G_\pm(\alpha)}{K_\pm(\alpha)} + \frac{1}{2\pi i}\int_{C_\pm} \frac{G_\mp(s) e^{\mp 2isL}}{(s-\alpha)K_\pm(s)} ds - \frac{1}{2\pi i}\int_{C_\pm} \frac{e^{\mp isL} K_\mp(s)}{\sqrt{2\pi}(s-\alpha)} \left\{ \frac{F_1}{\mu_1 \gamma_1(s)} - \frac{F_2}{\mu_2 \gamma_2(s)} \right\} ds = 0. \quad (41)$$

Since $\tau_{yz}^{(1)}(x,0)$ is an even function of x, so from (28) and (29) it can be shown that $G_+(-\alpha) = G_-(\alpha)$ and $K_+(-\alpha) = iK_-(\alpha)$ (cf. Pal and Ghosh [1990]). Using these results and replacing α by $-\alpha$ and s by -s in the first equation of (41) it can easily be shown that both the equations in (41) are identical. So $G_+(\alpha)$ and $G_-(\alpha)$ are to be determined from any one of the integral equations in (41).

3. HIGH FREQUENCY SOLUTION OF THE INTEGRAL EQUATION

To solve the second integral equation of (41) in the case when the normalized wave number $k_1L \gg 1$, the integration along the path C in (41) is replaced by the integration along the contours L_{k_1} and L_{k_2} around the branch cuts through the branch points k_1 and k_2 of the function $K_-(s)$ as shown in Fig.3. Thus the second equation in (41) takes the form

$$G_-(\alpha) = \frac{-K_-(\alpha)}{2\pi i}\int_{L_{k_1}+L_{k_2}} \frac{G_+(s)e^{2isL}}{(s-\alpha)K_-(s)}ds + \frac{K_-(\alpha)}{2\pi i}\int_{L_{k_1}+L_{k_2}} \frac{e^{isL}K_+(s)}{\sqrt{2\pi}(s-\alpha)}\left\{\frac{F_1}{\mu_1\gamma_1(s)} - \frac{F_2}{\mu_2\gamma_2(s)}\right\}ds. \quad (42)$$

For $k_1L \gg 1$, it can be shown that

$$\int_{L_{k_j}} \frac{G_+(s)e^{2isL}}{(s-\alpha)K_-(s)}ds \approx \frac{-1}{\mu_j}\sqrt{\frac{\pi}{k_jL}}\frac{G_+(k_j)K_+(k_j)}{(k_j-\alpha)}e^{i\pi/4}e^{2ik_jL}, \quad j=1,2, \quad (43)$$

and

$$\int_{L_{k_1}+L_{k_2}} \frac{K_+(s)}{\sqrt{2\pi}(s-\alpha)}\left\{\frac{F_1}{\mu_1\sqrt{(s^2-k_1^2)}} - \frac{F_2}{\mu_2\sqrt{(s^2-k_2^2)}}\right\}e^{isL}ds \approx \sum_{j=1}^{2}(-1)^j\frac{F_jK_+(k_j)e^{i(k_jL+\pi/4)}}{\mu_j(k_j-\alpha)\sqrt{k_jL}}. \quad (44)$$

Using the results of (43) and (44) and also the relations $G_+(-\alpha) = G_-(\alpha)$ and $K_-(\alpha) = -iK_+(-\alpha)$ one obtains from (42)

$$F_+(-\alpha) + \sum_{j=1}^{2}\frac{A(k_j)e^{2ik_jL}}{\mu_j(k_j-\alpha)\sqrt{k_jL}}F_+(k_j) = -C(-\alpha), \quad (45)$$

where

$$F_+(\xi) = \frac{G_+(\xi)}{K_-(-\xi)} = \frac{G_-(-\xi)}{K_-(-\xi)}, \quad (46)$$

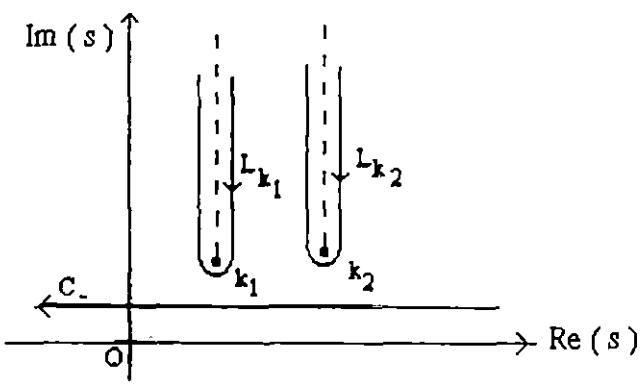

Fig.3. Path of integration C_-, L_{k_1}, L_{k_2}.

$$A(\xi) = \frac{[K_+(\xi)]^2 e^{i\pi/4}}{2\sqrt{\pi}}, \tag{47}$$

$$C(\xi) = \frac{1}{2\pi i}\sum_{j=1}^{2}(-1)^{j+1}\frac{F_j}{\mu_j}\frac{K_+(k_j)}{(k_j+\xi)}\frac{e^{i(k_jL+\pi/4)}}{\sqrt{k_jL}}. \tag{48}$$

Substituting $\alpha=-k_1$ and $\alpha=-k_2$ in (45) one obtains respectively the equations

$$\left[1 + M_1(k_1)e^{2ik_1L}\right]F_+(k_1) + \frac{\mu_1}{\mu_2}M_1(k_2)e^{2ik_2L}F_+(k_2) = -C(k_1) \tag{49}$$

and

$$\frac{\mu_2}{\mu_1}M_2(k_1)e^{2ik_1L}F_+(k_1) + \left[1 + M_2(k_2)e^{2ik_2L}\right]F_+(k_2) = -C(k_2), \tag{50}$$

where

$$M_j(\xi) = \frac{A(\xi)}{\mu_j(k_j+\xi)\sqrt{\xi L}}. \tag{51}$$

Now solution of (49) and (50) gives

$$F_+(k_m) = \left[\frac{\mu_m}{\mu_n}M_m(k_n)C(k_n)e^{2ik_nL} - C(k_m)\left\{1 + M_n(k_n)e^{2ik_nL}\right\}\right]P(k_1,k_2) \tag{52}$$

(for m=1, n=2 and for m=2, n=1)

where

$$P(k_1,k_2) = \left[1 + M_1(k_1)e^{2ik_1L} + M_2(k_2)e^{2ik_2L} + \left(\frac{k_1-k_2}{k_1+k_2}\right)^2 M_1(k_1)M_2(k_2)e^{2i(k_1+k_2)L}\right]^{-1}. \tag{53}$$

For high-frequency, expanding $P(k_1, k_2)$ up to $O(k_jL)^{-1}$ and neglecting the terms involving $(k_jL)^{-2}$ and the higher order terms in $F_+(k_1)$ and $F_+(k_2)$ in (52) respectively, one obtains from equations (45) and (46)

$$G_-(\alpha) = \frac{K_-(\alpha)}{2\pi i}\sum_{j=1}^{2}(-1)^jL(k_j)F_j\left\{\frac{1}{(k_j-\alpha)\mu_j} - \sum_{m=1}^{2}\frac{M_j(k_m)}{\mu_m(k_m-\alpha)}e^{2ik_mL} + \sum_{m=1}^{2}\sum_{n=1}^{2}\frac{M_j(k_m)M_m(k_n)}{\mu_n(k_n-\alpha)}e^{2i(k_m+k_n)L}\right\}, \tag{54}$$

where

$$L(\xi) = \frac{K_+(\xi)e^{i(\xi L+\pi/4)}}{\sqrt{\xi L}}. \tag{55}$$

Replacing α by $-\alpha$ and using the relations $K_-(-\alpha) = -iK_+(\alpha)$ and $G_-(-\alpha) = G_+(\alpha)$ one obtains,

$$G_+(\alpha) = -\frac{K_+(\alpha)}{2\pi}\sum_{j=1}^{2}(-1)^j L(k_j)F_j\left\{\frac{1}{(k_j+\alpha)\mu_j} - \sum_{m=1}^{2}\frac{M_j(k_m)}{\mu_m(k_m+\alpha)}e^{2ik_mL}\right.$$

$$\left. + \sum_{m=1}^{2}\sum_{n=1}^{2}\frac{M_j(k_m)M_m(k_n)}{\mu_n(k_n+\alpha)}e^{2i(k_m+k_n)L}\right\}. \qquad (56)$$

4. STRESS INTENSITY FACTOR NEAR THE CRACK TIPS

For $\alpha \to +\infty$ along the real axis,

$$K_\pm(\alpha) \sim \alpha^{1/2}\sqrt{\frac{\mu_1\mu_2}{\mu_1+\mu_2}}. \qquad (57)$$

From (53) and (56) one obtains,

$$G_+(\alpha) \sim S\,\alpha^{-1/2} \text{ and } G_-(\alpha) \sim -iS\,\alpha^{-1/2}, \qquad (58)$$

where

$$S = -\frac{1}{2\pi}\sqrt{\frac{\mu_1\mu_2}{\mu_1+\mu_2}}\sum_{j=1}^{2}(-1)^j L(k_j)F_j\left\{\frac{1}{\mu_j} - \sum_{m=1}^{2}\frac{M_j(k_m)}{\mu_m}e^{2ik_mL}\right.$$

$$\left. + \sum_{m=1}^{2}\sum_{n=1}^{2}\frac{M_j(k_m)M_m(k_n)}{\mu_n}e^{2i(k_m+k_n)L}\right\}. \qquad (59)$$

Using (57) and (58), equation (37) yields

$$B(\alpha) = \frac{S}{\alpha\sqrt{\alpha}}\left\{ie^{-i\alpha L} - e^{i\alpha L}\right\}\left(\frac{\mu_1+\mu_2}{\mu_1\mu_2}\right) + \frac{1}{\sqrt{2\pi}}\left\{\frac{F_1}{\mu_1} - \frac{F_2}{\mu_2}\right\}\frac{1}{\alpha}. \qquad (60)$$

From equations (18), (19) and (20) one obtains,

$$\tau_{yz}^{(1)}(x,0+) - \tau_{yz}^{(2)}(x,0-) = -(F_1+F_2)\delta(x).$$

Taking Fourier transformation on both sides, we obtain

$$\bar{\tau}_{yz}^{(1)}(\alpha,0+) - \bar{\tau}_{yz}^{(2)}(\alpha,0-) = -\frac{(F_1+F_2)}{\sqrt{2\pi}}$$

or

$$\mu_1\gamma_1 A_1(\alpha) + \mu_2\gamma_2 A_2(\alpha) = \frac{(F_1+F_2)}{\sqrt{2\pi}}. \qquad (61)$$

From equations (60), (61) and (36) one obtains when $\alpha \to +\infty$ along the real axis,

$$A_j(\alpha) = \frac{(-1)^{j+1} S}{\mu_j \alpha \sqrt{\alpha}} \left[i e^{-i\alpha L} - e^{i\alpha L} \right] + \frac{1}{\sqrt{2\pi}} \frac{1}{\alpha} \frac{F_j}{\mu_j}; \quad j=1,2. \tag{62}$$

Now

$$\tau_{yz}^{(j)}(x,y) = \mu_j \frac{\partial w_j(x,y)}{\partial y} = \mu_j \frac{\partial}{\partial y} \left[\frac{1}{\sqrt{2\pi}} \int_{-\infty}^{\infty} A_j(\alpha) e^{-\gamma_j |y| - i\alpha x} d\alpha \right]$$

$$= (-1)^j \frac{\mu_j}{\sqrt{2\pi}} \int_0^{\infty} \gamma_j A_j(\alpha) e^{-\gamma_j |y|} \left[e^{-i\alpha x} + e^{i\alpha x} \right] d\alpha \tag{63}$$

as by equation (35) $A_j(\alpha)$ is an even function of α.

Substituting the values of $A_j(\alpha)$ as $|\alpha| \to \infty$ we can write the stress in the vicinity of the crack tip as

$$\tau_{yz}^{(j)}(x,y) \approx \frac{S}{\sqrt{2\pi}} \int_0^{\infty} \frac{e^{-\alpha|y|}}{\sqrt{\alpha}} \left[e^{i\alpha(x+L)} - ie^{i\alpha(x-L)} - ie^{-i\alpha(x+L)} + e^{-i\alpha(x-L)} \right] d\alpha +$$

$$+ (-1)^j \frac{F_j}{\mu} \int_0^{\infty} e^{-\alpha|y|} \cos x\alpha \, d\alpha$$

$$= \frac{S(1-i)}{\sqrt{2\pi}} \int_0^{\infty} \frac{e^{-\alpha|y|}}{\sqrt{\alpha}} \left[\cos\alpha(x+L) - \sin\alpha(x+L) + \cos\alpha(x-L) + \sin\alpha(x-L) \right] d\alpha +$$

$$+ (-1)^j \frac{F_j}{\mu} \int_0^{\infty} e^{-\alpha|y|} \cos x\alpha \, d\alpha$$

$$= S(1-i) \left[\frac{1}{\sqrt{r_1}} \cos\frac{\theta_1}{2} + \frac{1}{\sqrt{r_2}} \cos\frac{\theta_2}{2} \right] + (-1)^j \frac{F_j}{\pi} \frac{|y|}{x^2+y^2}, \tag{64}$$

where

$$(x-L) + iy = r_1 e^{i\theta_1}, \qquad -(x+L) + iy = r_2 e^{i\theta_2}, \qquad -\pi \le \theta_{1,2} \le \pi. \tag{65}$$

It is to be noted that the final term in equation (64) which can be reduced to $-\frac{F_j}{\pi} \frac{y}{x^2+y^2}$ describes the behaviour of the stress near the source. Therefore at the interface (y=0) we obtain

$$\tau_{yz} \approx \frac{S(1-i)}{\sqrt{(x-L)}} \quad \text{as } x \to L+0, \tag{66}$$

$$\tau_{yz} \approx \frac{S(1-i)}{\sqrt{-(x+L)}} \quad \text{as } x \to -L-0. \tag{67}$$

Now the dimensionless stress intensity factor is defined by,

$$K = \left| \frac{S(1-i)}{F_1\sqrt{k_1}} \right|, \tag{68}$$

where S is given by (59).

5. RESULTS AND DISCUSSIONS

Since from equations (7) and (16) we note that for Y=0, x=X and y=0 and that $\sigma^{(j)}_{YZ}(X,0,t) = \sigma^{(j)}_{yz}(x,0,t)$, therefore, the elastodynamic mode-III stress intensity factor of the interface crack in an anisotropic bimaterials is the same as that of an interface crack of the corresponding isotropic bimaterial given by (68).

Numerical calculations have been carried out for both the cases of antisymmetric ($F_1 = -F_2 = F$) and symmetric ($F_1 = F_2 = F$) antiplane loadings. For numerical evalution of the stress intensity factors, the three material pairs (Nayfen, [1995]), given in Table-1, have been considered.

Table-1. Engineering elastic constants of different materials.

Medium	Name	$\hat{\rho}$(Kg m^{-3})	C_{44} (Gpa)	C_{55} (Gpa)	C_{45} (Gpa)
Type of material pair : I					
1.	Carbon-epoxy	1.57×10^3	3.98	6.4	0
2.	Graphite-epoxy	1.60×10^3	6.55	2.6	0
Type of material pair : II					
1.	Isotropic Chromium	7.20×10^3	115.2	115.2	0
2.	Isotropic Steel	7.90×10^3	81.91	81.91	0
Type of material pair : III					
1.	Graphite	1.79×10^3	5.52	28.3	0
2.	Carbon-epoxy	1.57×10^3	3.98	6.4	0

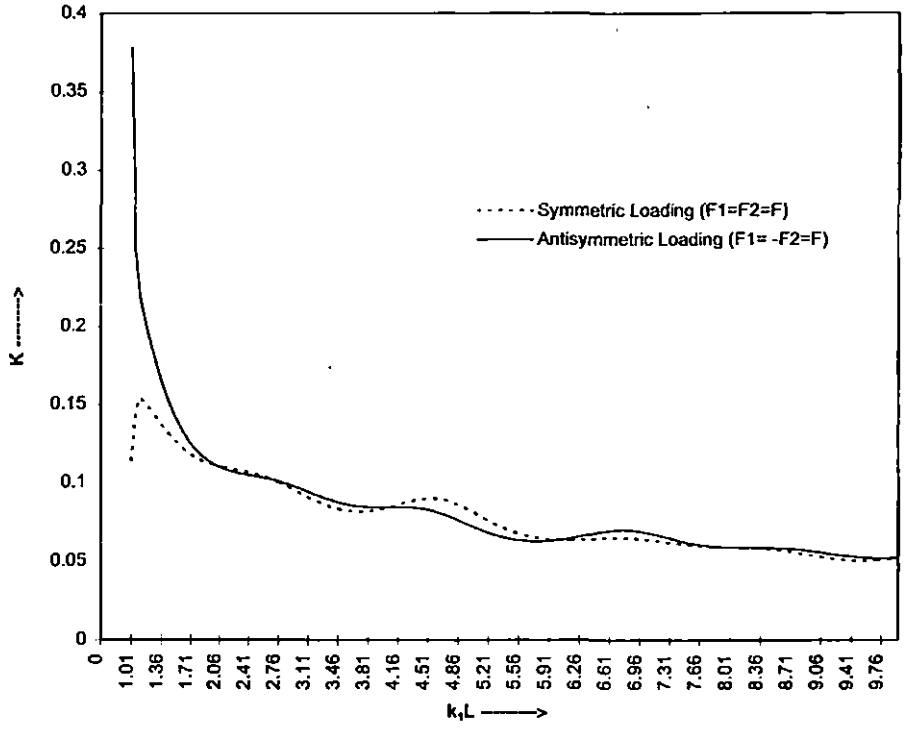

Fig.4. Stress intensity factor K versus dimensionless frequency k_1L for Type-I material pair.

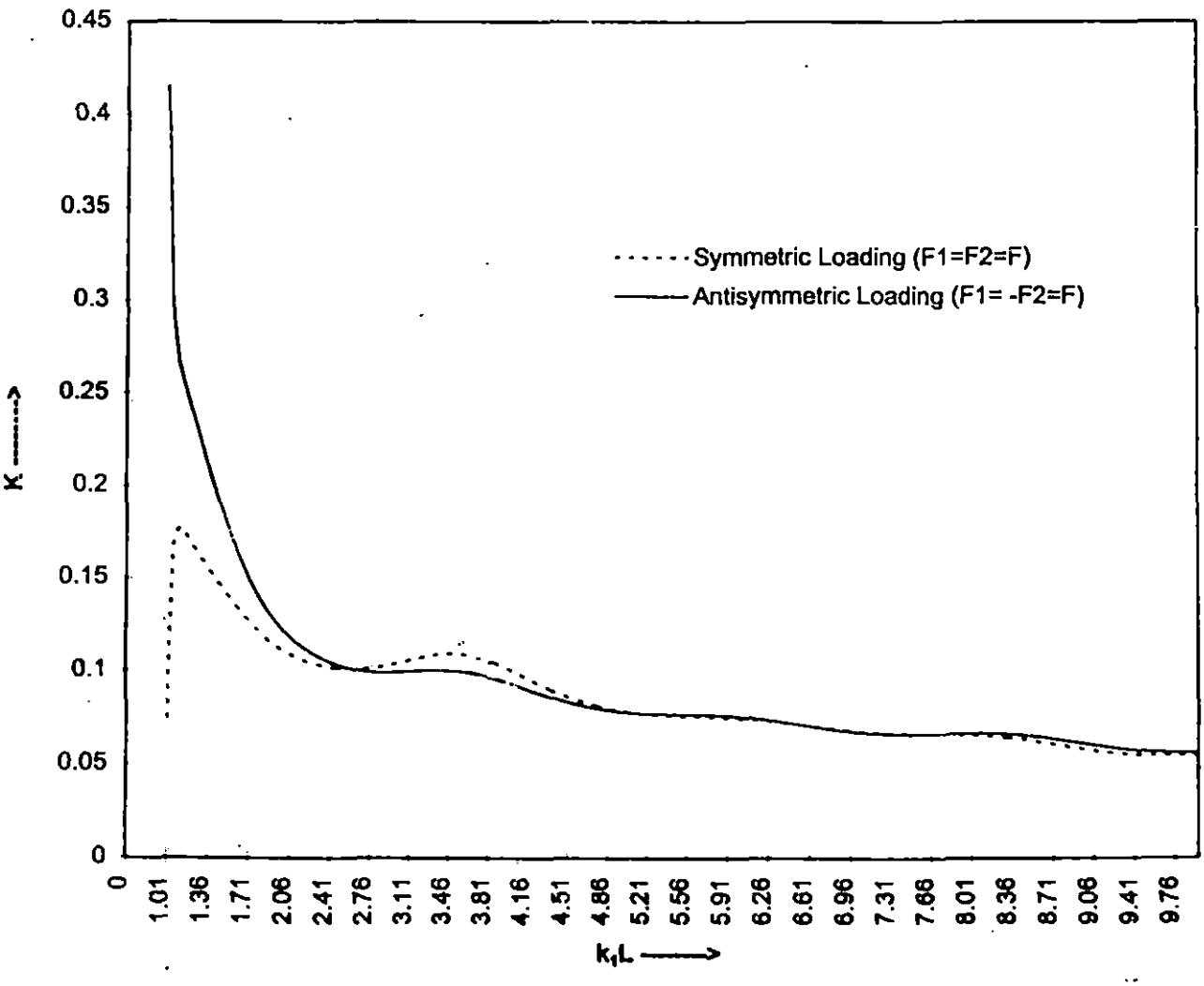

Fig.5. Stress intensity factor K versus dimensionless frequency k_1L for Type-II material pair.

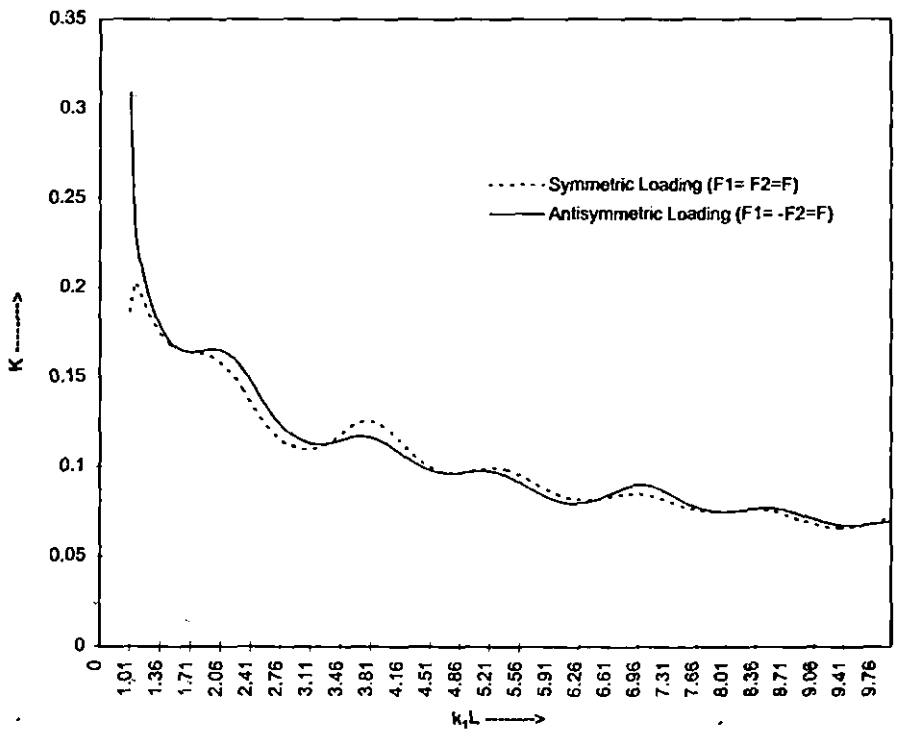

Fig.6. Stress intensity factor K versus dimensionless frequency k_1L for Type-III material pair.

The absolute values of the complex stress intensity factors defined by (68) have been plotted against k_1L in Figs. 4-6, for symmetric as well as for antisymmetric loadings for values of dimensionless frequency k_1L varying from 1.01 to 10.

It is interesting to note that in the case of symmetric loading, the stress intensity factor first increases with the increasing k_1L, attains a maximum and the with further increase of k_1L, decreases gradually with oscillatory behavior. On the other hand in the case of antisymmetric loading, stress intensity factor at first decreases sharply but with the increase of k_1L, it shows almost the same behaviours as the case for symmetric loading. The general oscillatory feature for the curves in Figs. 4-6 are due to the effect of interaction between the waves generated by the two tips of the crack.

----x----

[2]TRANSIENT RESPONSE DUE TO A PAIR OF ANTIPLANE POINT IMPACT LOADING ON THE FACES OF A FINITE GRIFFITH CRACK AT THE BIMATERIAL INTERFACE OF ANISOTROPIC SOLIDS

1. INTRODUCTION

The problem of a crack in an elastic material under the action of impulsive loading has been a subject of considerable interest recently. Sih et al [1972] have considered the problem for an infinite isotropic material and Kassir and Bandyopadhyay [1983] studied infinite orthotropic material. Stephen and Hwel [1970] also investigated the problem of diffraction of transient SH-waves by a crack of finite width and a rigid ribbon, also of finite width.

However in present years the extensive use of composite materials in the modern technology has created interest among scientists for carrying on considerable research work in the modeling, testing and analysis of laminated media. The laminated composites which behave as anisotropic material may be weakened by interface flaws which lead to serious degradation in load carrying capacity.

Kuo [1984] carried out numerical and analytical studies of transient response of an interfacial semi-infinite crack between two dissimilar orthotropic half spaces. The problem of diffraction of transient horizontal shear waves by a finite crack located at the interface of two bonded dissimilar elastic half spaces has been treated by Takei et al [1982].

Neerhoff [1979] studied the diffraction of Love waves by a crack of finite width at the interface of a layered half space. Kuo and Cheng [1991] considered the elastodynamic response due

---

[2] **Published in the Int. J. Engineering Science, V36, 1197-1213, 1998.**

to antiplane point impact loadings on the faces of an interface semi-infinite crack along dissimilar anisotropic materials.

In our present paper, we are interested in the antiplane transient elastodynamic responses and stress intensity factors of a Griffith crack of finite width lying along the interface of two dissimilar anisotropic elastic materials. The crack is subjected to a pair of suddenly applied antiplane concentrated line loading situated at the middle of the cracked surface. The materials are assumed to possess certain material symmetry and the crack plane is assumed to coincide with one of the planes of material symmetry, so that the inplane and the antiplane motion are not coupled.

The analysis of the paper is first based on the observation of several researches, e.g. Markenscoff and Ni [1984], Achenbach and Kuo [1981], that antiplane shear deformation in an anisotropic solid can be deduced from the corresponding deformations of an isotropic solid by a transformation of relevant co-ordinates and parameters. Based on this observation, analysis of the interface crack by transient line loads between two bonded dissimilar anisotropic elastic materials has first been converted to the corresponding problem between two dissimilar isotropic elastic solids. Later following Thau and Lu [1970], spatial and time transform are applied to the governing differential equations and generalized Wiener-Hopf type equations are obtained. The integral equation arising are solved by the standard iteration procedure. Physically, each successive order of iteration corresponds to successive scattered or rescattered wave from one crack tip to other.

Finally results are presented for the stress intensity factor near the crack tips. Each crack tip stress intensity factor is plotted versus time for a pair of different type of anisotropic materials.

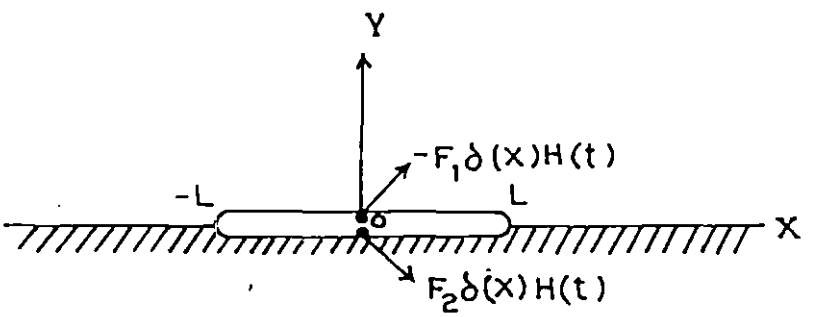

Fig.1. Geometry of the problem.

2. FORMULATION OF THE PROBLEM

Consider antiplane deformation of a Griffith crack of finite width 2L lying between dissimilar anisotropic half planes which are characterized by the elastic moduli $(C_{ik})_j$; (i,k=4,5) and mass density $\hat{\rho}_j$. The subscript j (j=1,2) refers to the upper and lower media respectively. Let (X,Y,Z) be the Cartesian co-ordinates. The X-axis is taken along the interface, Y-axis vertically upwards into the medium and Z-axis is perpendicular to the plane of the paper (Fig.1).

For time $t<0$, the elastic solids are at rest. For time $t\geq 0$, a pair of concentrated antiplane shear forces in the Z-direction of magnitudes F_1 and F_2 act on the crack faces Y=0+ and Y=0- respectively at X=0. Thus the crack boundary conditions are

$$\hat{\sigma}_{YZ}(X,Y,t) = \begin{cases} -F_1\,\delta(X)\,H(t); & |X|<L, \quad Y=0+, \\ F_2\,\delta(X)\,H(t); & |X|<L, \quad Y=0-, \end{cases} \qquad (1)$$

where H() and δ() are the Heaviside step and Dirac delta functions respectively. Ahead of the crack tips, the interface boundary conditions which corresponds to the continuity of the displacement and traction along the welded part of the interface along |X|>L, Y=0 are

$$\hat{\sigma}^{(1)}_{YZ}(X,0,t) = \hat{\sigma}^{(2)}_{YZ}(X,0,t) \qquad (2)$$

$$\hat{W}_1(X,0,t) = \hat{W}_2(X,0,t). \qquad (3)$$

Two dimensional antiplane wave motions of homogeneous anisotropic linearly elastic solids are governed by (Camprin [1981])

$$(C_{55})_j \frac{\partial^2 \hat{W}_j}{\partial X^2} + 2(C_{45})_j \frac{\partial^2 \hat{W}_j}{\partial X \partial Y} + (C_{44})_j \frac{\partial^2 \hat{W}_j}{\partial Y^2} = \hat{\rho}_j \frac{\partial^2 \hat{W}_j}{\partial t^2} \qquad (j=1,2), \qquad (4)$$

where $\hat{W}_j(X,Y,t)$ is the out-of-plane displacement.

The crack plane has been assumed to coincide with one of the planes of material symmetry such that inplane and out-plane motions are not coupled.

The relevant stress components are

$$\hat{\sigma}^{(j)}_{XZ}(X,Y,t) = (C_{55})_j \frac{\partial \hat{W}_j}{\partial X} + (C_{45})_j \frac{\partial \hat{W}_j}{\partial Y} \tag{5}$$

$$\hat{\sigma}^{(j)}_{YZ}(X,Y,t) = (C_{45})_j \frac{\partial \hat{W}_j}{\partial X} + (C_{44})_j \frac{\partial \hat{W}_j}{\partial Y}. \tag{6}$$

Following Achenbach and Kuo [1986] and Ma [1989], we introduce a co-ordinate transformation which has also been used by Kuo and Cheng [1991]

$$\left.\begin{aligned} x &= X - \frac{(C_{45})_j}{(C_{44})_j} Y, \\ y &= \frac{\mu_j}{(C_{44})_j} Y, \\ z &= Z, \end{aligned}\right\} \qquad (j = 1, 2) \tag{7}$$

where

$$\mu_j = \sqrt{(C_{44})_j (C_{55})_j - (C_{45})_j^2} \qquad (j = 1, 2). \tag{8}$$

Transformation given by equation (7) reduce equation (4) to the standard wave equation

$$\frac{\partial^2 \hat{W}_j}{\partial x^2} + \frac{\partial^2 \hat{W}_j}{\partial y^2} = s_j^2 \frac{\partial^2 \hat{W}_j}{\partial t^2}, \tag{9}$$

where

$$s_j^2 = \frac{\rho_j}{\mu_j} \quad \text{and} \quad \rho_j = \frac{\hat{\rho}_j (C_{44})_j}{\mu_j}, \tag{10}$$

s_j is the slowness of shear waves. Without any loss of generality we assume that

$$s_1 < s_2 . \tag{11}$$

It is easily verified from equations (4) - (6) that the relevant displacement and the stress component in the physical anisotropic solid are related to those in the corresponding isotropic solid by

$$\hat{W}_j (X, Y, t) = w_j(x, y, t), \tag{12}$$

$$\hat{\sigma}^{(j)}_{XZ} (X, Y, t) = \frac{\mu_j}{(C_{44})_j} \sigma^{(j)}_{xz}(x, y, t) + \frac{(C_{45})_j}{(C_{44})_j} \sigma^{(j)}_{yz}(x, y, t), \tag{13}$$

$$\hat{\sigma}^{(j)}_{YZ} (X, Y, t) = \sigma^{(j)}_{yz}(x, y, t). \tag{14}$$

From equations (9) and (12), the antiplane wave motions of the corresponding isotropic bimaterial in the transformed co-ordinate are governed by the standard wave equation

$$\frac{\partial^2 w_j}{\partial x^2} + \frac{\partial^2 w_j}{\partial y^2} = s_j^2 \frac{\partial^2 w_j}{\partial t^2}; \qquad (j = 1, 2) \tag{15}$$

and the relevant stress components are

$$\sigma^{(j)}_{yz}(x, y, t) = \mu_j \frac{\partial w_j}{\partial y}. \tag{16}$$

Under the changed co-ordinate system the boundary conditions equations (1) - (3) reduce to

$$\sigma_{yz}(x,y,t) = \begin{cases} -F_1\,\delta(x)\,H(t); & |x|<L, \quad y=0+ \\ F_2\,\delta(x)\,H(t); & |x|<L, \quad Y=0- \end{cases} \tag{17}$$

$$\sigma_{yz}^{(1)}(x,y,t) = \sigma_{yz}^{(2)}(x,y,t); \qquad |x|>L, \quad y=0, \tag{18}$$

$$w_1(x,y,t) = w_2(x,y,t); \qquad |x|>L, \quad y=0. \tag{19}$$

Hence

$$\mu_1 \frac{\partial w_1}{\partial y} = -F_1\,\delta(x)\,H(t); \qquad |x|<L, \quad y=0+ \tag{20}$$

$$\mu_2 \frac{\partial w_2}{\partial y} = F_2\,\delta(x)\,H(t); \qquad |x|<L, \quad y=0- \tag{21}$$

and

$$\mu_1 \frac{\partial w_1}{\partial y} = \mu_2 \frac{\partial w_2}{\partial y}; \qquad |x|>L, \quad y=0 \tag{22}$$

$$w_1(x,0,t) = w_2(x,0,t); \qquad |x|>L, \quad y=0. \tag{23}$$

We begin the analysis by introducing unknown functions w_j and $\partial w_j / \partial y$ along the x-axis over the intervals where the functions are not specified by equations (22) and (23).

Assume that

$$w_j(x,0,t) = g_j(x,0,t); \qquad -L<x<L \tag{24}$$

and

$$\mu_j \frac{\partial w_j}{\partial y} = \begin{cases} \phi(x+L,t); & y=0, \quad x+L<0 \\ \phi(x-L,t); & y=0, \quad x-L>0 \end{cases} . \tag{25}$$

Now we introduce Laplace anf Fourier transforms defined as

$$F(x,y,p) = \int_0^\infty f(x,y,t)\, e^{-pt} dt, \qquad \bar{F}(\zeta,y,p) = \int_{-\infty}^{\infty} F(x,y,p) e^{-i\zeta x} dx \tag{26}$$

so that their inverse transforms are

$$f(x,y,t) = \frac{1}{2\pi i} \int_{BR} F(x,y,p) e^{pt} dp, \qquad F(x,y,p) = \frac{1}{2\pi} \int_{-\infty}^{\infty} \bar{F}(\zeta,y,p)\, e^{i\zeta x} d\zeta . \tag{27}$$

Taking Laplace transform with respect to t of both sides of equation (24) (for $|x| < L$)

$$W_j(x,0,p) = \int_0^\infty w_j(x,0,t) e^{-pt} dt = \int_0^\infty g_j(x,0,t) e^{-pt} dt = G_j(x,0,p); \quad |x|<L. \tag{28}$$

Next taking Laplace and Fourier transform on wave equation (15) one obtains

$$\frac{\partial^2 \bar{w}_1}{dy^2} - (\zeta^2 + k_1^2)\bar{w}_1 = 0; \qquad y>0, \tag{29}$$

$$\frac{\partial^2 \bar{w}_2}{dy^2} - (\zeta^2 + k_2^2)\bar{w}_2 = 0; \qquad y<0, \tag{30}$$

where

$$k_j^2 = s_j^2 p^2; \qquad (j=1,2). \tag{31}$$

The solutions of equations (29) and (30) which are bounded as $|y| \to \infty$ are

$$\bar{w}_1(\zeta,y,p) = A_1(\zeta)e^{-\gamma_1 y}; \qquad y>o, \tag{32}$$

$$\bar{w}_2(\zeta,y,p) = A_2(\zeta)e^{\gamma_2 y}; \qquad y<o, \tag{33}$$

where

$$\gamma_j = \sqrt{(\zeta^2 + k_j^2)}; \qquad (j=1,2). \tag{34}$$

The transformed stress at the interface y=0 can be written as

$$\mu_j \frac{\partial \bar{W}_j(\zeta,0,p)}{\partial y} = e^{i\zeta L}\bar{\Phi}_+(\zeta,p) + \frac{1}{p}\epsilon_j F_j + e^{-i\zeta L}\bar{\Phi}_-(\zeta,p), \quad [j=1,2, \quad \epsilon_j=(-1)^j], \tag{35}$$

where

$$\bar{\Phi}_+(\zeta,p) = \int_{-\infty}^{-L} e^{-i\zeta x}\left[\int_0^{\infty} \phi(x+L,t)e^{-pt}dt\right]dx$$

and

$$\bar{\Phi}_-(\zeta,p) = \int_{L}^{\infty} e^{-i\zeta x}\left[\int_0^{\infty} \phi(x-L,t)e^{-pt}dt\right]dx.$$

$\bar{\Phi}_+$ and $\bar{\Phi}_-$ are analytic in the complex half plane $\mathrm{Im}(\zeta) > -k_1$ and $\mathrm{Im}(\zeta) < k_1$ respectively. So from equations (32) and (33) one obtains

$$\mu_1 \frac{\partial \bar{W}_1(\zeta,0,p)}{\partial y} = -\mu_1\gamma_1 A_1(\zeta), \qquad \mu_2 \frac{\partial \bar{W}_2(\zeta,0,p)}{\partial y} = \mu_2\gamma_2 A_2(\zeta). \tag{36}$$

Equation (35) with aid of equation (36) yields

$$(-1)^j \mu_j\gamma_j A_j(\zeta) = e^{i\zeta L}\bar{\Phi}_+(\zeta,p) + e^{-i\zeta L}\bar{\Phi}_-(\zeta,p) + (-1)^j \frac{F_j}{p}; \quad (j=1,2). \tag{37}$$

Taking aid of equations (19), (28), (32) and (33) one obtains

$$\bar{W}_1(\zeta,0,p) - \bar{W}_2(\zeta,0,p) = \int_{-\infty}^{\infty} \{W_1(x,0,p) - W_2(x,0,p)\} e^{-i\zeta x}\, dx$$

$$= \int_{-L}^{L} \{G_1(x,0,p) - G_2(x,0,p)\} e^{-i\zeta x}\, dx = B(\zeta) \quad \text{(say)}$$

so that

$$A_1(\zeta) - A_2(\zeta) = B(\zeta). \tag{38}$$

By the help of equations (37) and (38) one finds an extended Wiener-Hopf equation namely

$$K(\zeta)B(\zeta) = -\bar{\Phi}_+(\zeta,p)\, e^{i\zeta L} + \bar{\Phi}_-(\zeta,p)\, e^{-i\zeta L} + \frac{K(\zeta)}{p}\left\{\frac{F_1}{\mu_1\gamma_1} - \frac{F_2}{\mu_2\gamma_2}\right\}, \tag{39}$$

where

$$K(\zeta) = \frac{\mu_1\mu_2\gamma_1\gamma_2}{\mu_1\gamma_1 + \mu_2\gamma_2} = \frac{\mu_1\mu_2\sqrt{\zeta^2 + k_1^2}}{\mu_1 + \mu_2} R^1(\zeta) \tag{40}$$

$$= \frac{\mu_1\mu_2\sqrt{\zeta^2 + k_2^2}}{\mu_1 + \mu_2} R^2(\zeta) \tag{41}$$

so that

$$R^{1}(\zeta) = \frac{(\mu_1+\mu_2)\sqrt{(\zeta_2+k_2^2)}}{\mu_1\sqrt{(\zeta_2+k_1^2)}+\mu_2\sqrt{(\zeta_2+k_2^2)}}, \tag{42}$$

$$R^{2}(\zeta) = \frac{(\mu_1+\mu_2)\sqrt{(\zeta_2+k_1^2)}}{\mu_1\sqrt{(\zeta_2+k_1^2)}+\mu_2\sqrt{(\zeta_2+k_2^2)}}. \tag{43}$$

The solution of equation (39) along with two transform inversions completes the problem. Here we shall concentrate on finding and then inverting $\bar{\Phi}_+$ and $\bar{\Phi}_-$ since $\phi(x+L, t)$ and $\phi(x-L,t)$ from equation (25) are equal to the shear stresses directly ahead of the crack tips. Hence they are required for the determination of dynamic stress intensity factors at the crack tips.

In order to solve equation (39), the function $K(\zeta)$ is at first made single valued by drawing branch cuts along the η-axis (recall $\zeta=\xi+i\eta$) from $\eta=k_1$ to ∞ and from $\eta=-k_1$ to $-\infty$. It is then broken up into the product of two functions which are analytic in the overlapping regions $Im(\zeta)>-k_1$ and $Im(\zeta)<k_1$ so that

$$K(\zeta) = K_+(\zeta)\,K_-(\zeta). \tag{44}$$

Next we divide equation (39) by $K_+(\zeta)$ and change ζ to ζ' in it and redivide it by $2\pi i e^{i\zeta' L}(\zeta'-\zeta)$ which yields

$$\frac{e^{-i\zeta' L}K_-(\zeta')B(\zeta')}{2\pi i(\zeta'-\zeta)} = -\frac{\bar{\Phi}_+(\zeta')}{2\pi i K_+(\zeta')(\zeta'-\zeta)} + \frac{\bar{\Phi}_-(\zeta')e^{-2i\zeta' L}}{2\pi i K_+(\zeta')(\zeta'-\zeta)}$$

$$+\frac{K_-(\zeta')e^{-i\zeta' L}}{2\pi i(\zeta'-\zeta)p}\left[\frac{F_1}{\mu_1\sqrt{(\zeta'^2+k_1^2)}}-\frac{F_2}{\mu_2\sqrt{(\zeta'^2+k_2^2)}}\right]. \tag{45}$$

Now with $\zeta'=\xi'+i\eta'$, take a line L_1 in the ζ'-plane lying in the strip $-k_1<\eta'<k_1$; choose

ζ to be a point lying above L_1 (i.e. $\eta>\eta'$) and integrate equation (45) along L_1 from $-\infty<\xi'<\infty$

$$\int_{L_1}\frac{e^{-i\zeta' L}K_-(\zeta')B(\zeta')}{2\pi i(\zeta'-\zeta)}d\zeta' = -\int_{L_1}\frac{\bar{\Phi}_+(\zeta')}{2\pi i K_+(\zeta')(\zeta'-\zeta)}d\zeta' + \int_{L_1}\frac{\bar{\Phi}_-(\zeta')e^{-2i\zeta' L}}{2\pi i K_+(\zeta')(\zeta'-\zeta)}d\zeta'$$

$$+\int_{L_1}\frac{K_-(\zeta')e^{-i\zeta' L}}{2\pi i(\zeta'-\zeta)p}\left[\frac{F_1}{\mu_1\sqrt{(\zeta'^2+k_1^2)}}-\frac{F_2}{\mu_2\sqrt{(\zeta'^2+k_2^2)}}\right]d\zeta'. \qquad (46)$$

Since $B(\zeta')$ is analytic in the entire plane and $K_-(\zeta')e^{-i\zeta' L}$ is analytic in the lower half plane, so considering semicircular contour in the lower half plane the first integral is found to be equal to zero.

Again while evaluating the second integral, a semicircular contour in the upper half plane is considered. Consequently the second integral is found to yield the value $\bar{\Phi}_+(\zeta)/K_+(\zeta)$.

Next for the last two integrals the integration path is deformed to the path round the branch cut through the branch points $\zeta = -ik_1$ and $-ik_2$ as shown in Fig.2 so that finally equation (46) takes the form

$$\bar{\Phi}_+(\zeta) = \frac{iK_+(\zeta)}{\pi\mu_1}\int_0^\infty \frac{\bar{\Phi}_-[-ik_1(1+\lambda)]\,K_-[-ik_1(1+\lambda)]\,e^{-2Lk_1(1+\lambda)}}{[ik_1(1+\lambda)+\zeta]\sqrt{\lambda(\lambda+2)}}d\lambda$$

$$+\frac{iK_+(\zeta)}{\pi\mu_2}\int_0^\infty \frac{\bar{\Phi}_-[-ik_2(1+\lambda)]\,K_-[-ik_2(1+\lambda)]\,e^{-2Lk_2(1+\lambda)}}{[ik_2(1+\lambda)+\zeta]\sqrt{\lambda(\lambda+2)}}d\lambda$$

$$+\frac{iF_1K_+(\zeta)}{\pi\mu_1 p}\int_0^\infty \frac{K_-[-ik_1(1+\lambda)]\,e^{-Lk_1(1+\lambda)}}{[ik_1(1+\lambda)+\zeta]\sqrt{\lambda(\lambda+2)}}d\lambda$$

$$-\frac{iF_2K_+(\zeta)}{\pi\mu_2 p}\int_0^\infty \frac{K_-[-ik_2(1+\lambda)]\,e^{-Lk_2(1+\lambda)}}{[ik_2(1+\lambda)+\zeta]\sqrt{\lambda(\lambda+2)}}d\lambda. \qquad (47)$$

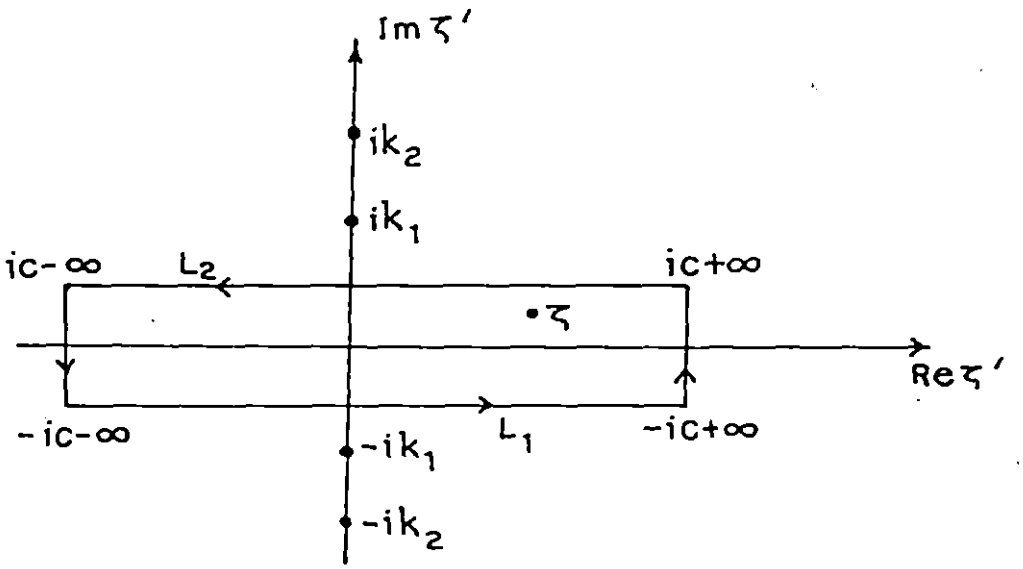

Fig.2. Path of integration.

Similarly we can derive an equation for $\bar{\Phi}_-(\zeta)$ by dividing equation (39) by $2\pi i e^{-2\zeta' L} K_-(\zeta')(\zeta'-\zeta)$ after first changing ζ to ζ' and then choosing a line of integration L_2 in the strip $-k_1<\eta'<k_1$. The point ζ is taken below L_2 and the result analogous to equation (47), then becomes;

$$\bar{\Phi}_-(\zeta) = \frac{iK_-(\zeta)}{\pi\mu_1}\int_0^\infty \frac{\bar{\Phi}_+[ik_1(1+\lambda)]\,K_+[ik_1(1+\lambda)]\,e^{-2Lk_1(1+\lambda)}}{[ik_1(1+\lambda)-\zeta]\sqrt{\lambda(\lambda+2)}}\,d\lambda$$

$$+\frac{iK_-(\zeta)}{\pi\mu_2}\int_0^\infty \frac{\bar{\Phi}_+[ik_2(1+\lambda)]\,K_+[ik_2(1+\lambda)]\,e^{-2Lk_2(1+\lambda)}}{[ik_2(1+\lambda)-\zeta]\sqrt{\lambda(\lambda+2)}}\,d\lambda$$

$$-\frac{iF_1K_-(\zeta)}{\pi\mu_1 p}\int_0^\infty \frac{K_+[ik_1(1+\lambda)]\,e^{-Lk_1(1+\lambda)}}{[ik_1(1+\lambda)-\zeta]\sqrt{\lambda(\lambda+2)}}\,d\lambda$$

$$+\frac{iF_2K_-(\zeta)}{\pi\mu_2 p}\int_0^\infty \frac{K_+[ik_2(1+\lambda)]\,e^{-Lk_2(1+\lambda)}}{[ik_2(1+\lambda)-\zeta]\sqrt{\lambda(\lambda+2)}}\,d\lambda. \qquad (48)$$

The integral equations have been solved by the standard iteration method and it may be noted that each successive order of iteration is a solution of the problem for successively increasing units of time starting from t=0. Since each unit of time here corresponds exactly to the time required for an SH-wave to traverse the crack width, we can interpret physically each order of iteration in terms of the successive scatterings of waves from one crack to other and back again. Now we consider the zeroth order solutions of equations (47) and (48) as

$$\bar{\Phi}_+^{(0)}(\zeta) = \frac{iF_1K_+(\zeta)e^{-Lk_1}}{\pi\mu_1 p}\int_0^\infty \frac{K_-[-ik_1(1+\lambda)]\,e^{-Lk_1\lambda}}{[ik_1(1+\lambda)+\zeta]\sqrt{\lambda(\lambda+2)}}\,d\lambda$$

$$-\frac{iF_2K_+(\zeta)e^{-Lk_2}}{\pi\mu_2 p}\int_0^\infty \frac{K_-[ik_2(1+\lambda)]\,e^{-Lk_2\lambda}}{[ik_2(1+\lambda)+\zeta]\sqrt{\lambda(\lambda+2)}}\,d\lambda \qquad (49)$$

and

$$\bar{\Phi}_-^{(0)}(\zeta) = -\frac{iF_1K_-(\zeta)e^{-Lk_1}}{\pi\mu_1 p}\int_0^\infty \frac{K_+[ik_1(1+\lambda)]\,e^{-Lk_1\lambda}}{[ik_1(1+\lambda)-\zeta]\sqrt{\lambda(\lambda+2)}}\,d\lambda$$

$$+\frac{iF_2K_-(\zeta)e^{-Lk_2}}{\pi\mu_2 p}\int_0^\infty \frac{K_+[ik_2(1+\lambda)]\,e^{-Lk_2\lambda}}{[ik_2(1+\lambda)-\zeta]\sqrt{\lambda(\lambda+2)}}\,d\lambda. \qquad (50)$$

Due to the presence of exponentially decaying terms in the integrands the main contribution to the integrals would be from small values of λ. So approximately evaluating the integrals we obtain finally

$$\bar{\Phi}_+^{(0)}(\zeta) = \frac{F_1K_+(\zeta)K_+(ik_1)e^{-Lk_1}}{\mu_1 p(\zeta+ik_1)\sqrt{2\pi Lk_1}} - \frac{F_2K_+(\zeta)K_+(ik_2)e^{-Lk_2}}{\mu_2 p(\zeta+ik_2)\sqrt{2\pi Lk_2}}, \qquad (51a)$$

$$\bar{\Phi}_-^{(0)}(\zeta) = \frac{iF_1K_-(\zeta)K_+(ik_1)e^{-Lk_1}}{\mu_1 p(\zeta-ik_1)\sqrt{2\pi Lk_1}} - \frac{iF_2K_-(\zeta)K_+(ik_2)e^{-Lk_2}}{\mu_2 p(\zeta-ik_2)\sqrt{2\pi Lk_2}}. \qquad (51b)$$

The expression for $\bar{\Phi}_+^{(0)}(\zeta)$ and $\bar{\Phi}_-^{(0)}(\zeta)$ may be recognised as the solutions corresponding to the separate problems of diffraction of semi-infinite cracks y=0, x>-L and y=0, x<L respectively because until the scattered wave emanating from a given crack tip reaches the opposite crack tip, the semi-infinite crack solution must apply.

The waves originating from concentrated line sources at x=0, y=0+ and x=0, y=0- arrive at the crack edges at $t=s_1L$ and $t=s_2L$ respectively.

The waves arriving at one edge at time $t=s_1L$ and $t=s_2L$ respectively through the upper and lower media reach the opposite edge at times $t=3s_1L$, s_2L+2s_1L through the upper medium and at time $t=s_1L+2s_2L$, $3s_2L$ through the lower medium. So the first order solution $\bar{\Phi}_+^{(1)}(\zeta)$ and $\bar{\Phi}_-^{(1)}(\zeta)$ which we obtain by substituting equations (51a - b) into the integral equations (47) and (48) gives

the effect of these waves and it is valid until $t=5s_1L$ when the second scattered wave from the opposite edge first arrives. So the first order iteration becomes

$$\bar{\Phi}_+^{(1)}(\zeta) = \sum_{r=1}^{2} \frac{K_+(\zeta)\bar{\Phi}_-^{(0)}(-ik_r)K_+(ik_r)e^{-2Lk_r}}{2\mu_r(\zeta+ik_r)\sqrt{\pi Lk_r}} - \sum_{r=1}^{2} \frac{(-1)^r F_r K_+(\zeta)K_+(ik_r)e^{-Lk_r}}{\mu_r p(\zeta+ik_r)\sqrt{2\pi Lk_r}} \quad (52a)$$

and

$$\bar{\Phi}_-^{(1)}(\zeta) = -i\sum_{r=1}^{2} \frac{K_-(\zeta)\bar{\Phi}_+^{(0)}(ik_r)K_+(ik_r)e^{-2Lk_r}}{2\mu_r(\zeta-ik_r)\sqrt{\pi Lk_r}} - i\sum_{r=1}^{2} \frac{(-1)^r F_r K_-(\zeta)K_+(ik_r)e^{-Lk_r}}{\mu_r p(\zeta-ik_r)\sqrt{2\pi Lk_r}}. \quad (52b)$$

For stress intensity factor since we are interested in the singular part of the stress near the crack tip, so making $|\zeta|\to\infty$ and noting that $R_+^{1,2}(\zeta)$ tends to unity as $|\zeta|\to\infty$ we obtain

$$\bar{\Phi}_+^{(1)}(\zeta) = \sqrt{\frac{\mu_1\mu_2}{\mu_1+\mu_2}}\left[\sum_{r=1}^{2} \frac{\bar{\Phi}_-^{(0)}(-ik_r)K_+(ik_r)e^{-2Lk_r}}{2\mu_r\sqrt{(\zeta+ik_r)}\sqrt{\pi Lk_r}} - \sum_{r=1}^{2} \frac{(-1)^r F_r K_+(ik_r)e^{-Lk_r}}{\mu_r p\sqrt{(\zeta+ik_r)}\sqrt{2\pi Lk_r}}\right] \quad (53a)$$

and

$$\bar{\Phi}_-^{(1)}(\zeta) = \sqrt{\frac{\mu_1\mu_2}{\mu_1+\mu_2}}\, i\left[-\sum_{r=1}^{2} \frac{\bar{\Phi}_+^{(0)}(ik_r)K_+(ik_r)e^{-2Lk_r}}{2\mu_r\sqrt{(\zeta-ik_r)}\sqrt{\pi Lk_r}} - \sum_{r=1}^{2} \frac{(-1)^r F_r K_+(ik_r)e^{-Lk_r}}{\mu_r p\sqrt{(\zeta-ik_r)}\sqrt{2\pi Lk_r}}\right]. \quad (53b)$$

Taking inverse Fourier transform we obtain,

$$\Phi_\pm(x\pm L) = \pm\left(\frac{\mu_1\mu_2}{\mu_1+\mu_2}\right)^2 \frac{1}{2\pi\sqrt{(L|x\pm L|)}}\left[-\frac{F_1[R_+^1(ik_1)]^3 e^{s_1 p(\pm x-2L)}}{\mu_1^2\sqrt{\mu s_1 L}\, p^{3/2}}\right.$$

$$\left. + \frac{F_2}{\mu_1\mu_2}\frac{R_+^1(ik_1)R_+^1(ik_2)R_+^2(ik_1)}{\sqrt{\pi s_2 L}}\frac{e^{p(\pm s_1 x - s_1 L - s_2 L)}}{p^{3/2}}\right.$$

$$- \frac{F_1}{\mu_1\mu_2}\frac{R_+^2(ik_2)R_+^2(ik_1)R_+^1(ik_2)}{\sqrt{\pi s_1 L}}\frac{e^{p(\pm s_2 x - s_1 L - s_2 L)}}{P^{3/2}}$$

$$+ \frac{F_2}{\mu_2^2}\frac{[R_+^2(ik_2)]^3}{\sqrt{\pi s_2 L}}\frac{e^{s_2 p(\pm x - 2L)}}{p^{3/2}}\Bigg]$$

$$\pm \frac{1}{\pi}\left(\frac{\mu_1\mu_2}{\mu_1+\mu_2}\right)\frac{1}{\sqrt{(L|x\pm L|)}}\sum_{r=1}^{2}\frac{(-1)^{r+1}F_r R_+^1(ik_r)e^{\pm s_r x p}}{\mu_r p} \quad \text{as } x\to\mp(L+0). \qquad (54)$$

Next from equation (54) the normalized stress intensity factors $K_{\pm L}(t)$ where subscripts -L, +L refer to the corresponding values at the crack tips at x=-L and x=L respectively have been derived.

Noting that $R_+^{1,2}(ik_1)$ and $R_+^{1,2}(ik_2)$ are independent of p and using shifting theorem, the inverse Laplace transform finally gives the normalised dynamic stress intensity factors as

$$|K_{\mp L}(t)| = \left|\frac{1}{F_1}\underset{x\to\mp L}{Lt}\frac{\phi(x\pm L)}{\sqrt{(L|x\pm L|)}}\right| = \left|-\frac{1}{\pi(1+m)}\left[mR_+^1(ik_1)H(\tau-1) - \frac{F_2}{F_1}R_+^2(ik_2)H(\tau-\gamma)\right]\right.$$

$$+ \frac{1}{\pi^2(1+m)^2}\Big[m^2[R_+^1(ik_1)]^3\sqrt{\tau-3}\,H(\tau-3)$$

$$- \frac{F_2}{F_1}mR_+^1(ik_1)R_+^1(ik_2)R_+^2(ik_1)\sqrt{\left(\frac{\tau}{\gamma}-\frac{2}{\gamma}-1\right)}\,H(\tau-2-\gamma)$$

$$+ mR_+^2(ik_2)R_+^2(ik_1)R_+^1(ik_2)\sqrt{(\tau-2\gamma-1)}\,H(\tau-2\gamma-1)$$

$$\left.- \frac{F_2}{F_1}[R_+^2(ik_2)]^3\sqrt{\left(\frac{\tau}{\gamma}-3\right)}\,H(\tau-3\gamma)\Big]\right|, \quad 1<\tau<5, \qquad (55)$$

where

$$m = \frac{\mu_2}{\mu_1}, \quad \gamma = \frac{s_2}{s_1} \quad \text{and} \quad \tau = \frac{t}{s_1 L}.$$

It may be noted that stress intensity factors at the both edges $|K_{+L}(t)|$ and $|K_{-L}(t)|$ are the same which is also obvious from the symmetry of the problem.

3. RESULTS AND DISCUSSIONS

From equations (7) and (14) it is to be noted that Y=0, x=X and y=0 and that $\hat{\sigma}^{(j)}_{YZ}(X,0,t) = \sigma^{j}_{yz}(x,0,t)$.

Therefore, elastodynamic mode III stress intensity factors at the crack tips of the interface crack in an anisotropic bimaterial are the same as that of the interface crack of the corresponding isotropic bimaterial given by equation (55).

While carrying out numerical calculations both the cases of symmetric ($F_1 = F_2 = F$) and antisymmetric ($F_1 = -F_2 = F$) loading have been treated. For numerical evaluation of stress intensity factors at the tips of the cracks of finite width situated at the interface, the four material pairs (Nayfeh [1995]), given in Table-1, have been considered.

The absolute value of the stress intensity factors defined by equation (55) has been plotted against $\tau \left(= \frac{t}{s_1 L} \right)$ for different material pairs in Figs. 3 - 6 for both the symmetric and antisymmetric loading for values of τ varying from 1.0 to 5.0.

It is to be noted that in the case of antisymmetric loading, stress intensity factor increases in two steps, the first step corresponds to the first arrival of the wave at the crack tip moving along the upper face of the crack from the source and the second jump occurring because of the arrival of the wave at the crack tip due to wave moving along the lower face of the crack.

Table-1. Engineering elastic constants of different materials.

Medium	Name	$\hat{\rho}$ (Kg m $^{-3}$)	C_{44} (Gpa)	C_{55} (Gpa)	C_{45} (Gpa)
Type of material pair : I					
1.	Carbon-epoxy	1.57×10^3	3.98	6.4	0
2.	Graphite-epoxy	1.60×10^3	6.55	2.6	0
Type of material pair : II					
1.	Isotropic Chromium	7.20×10^3	115.2	115.2	0
2.	Isotropic Steel	7.90×10^3	81.91	81.91	0
Type of material pair : III					
1.	Isotropic Aluminium	2.70×10^3	26.45	26.45	0
2.	Carbon-epoxy	1.57×10^3	3.98	6.4	0
Type of material pair : IV					
1.	Copper coated Stainless Steel	8.00×10^3	91	135	0
2.	Isotropic Aluminium	2.70×10^3	26.45	26.45	0

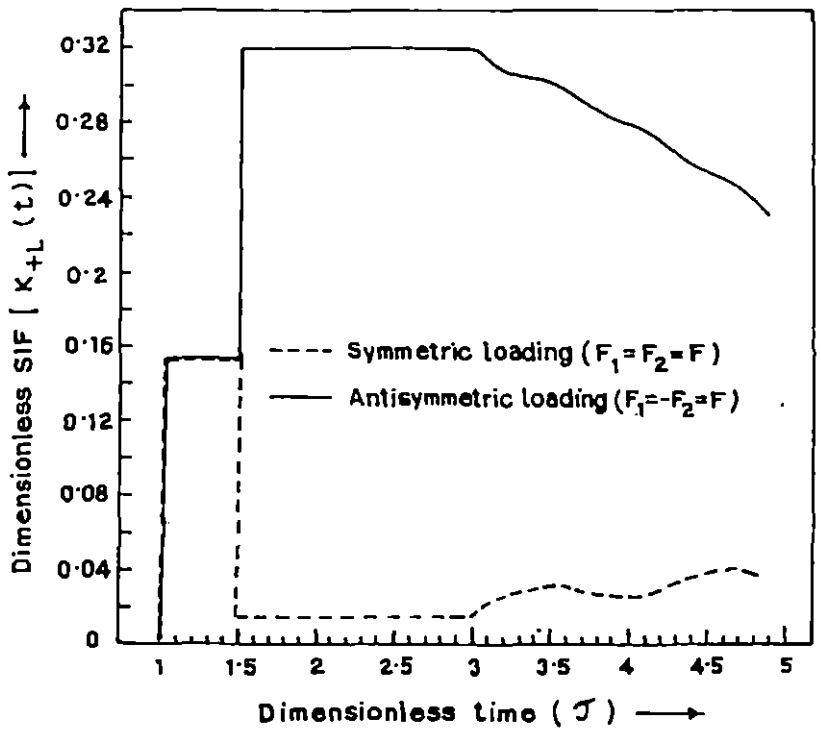

Fig.3. Stress intensity factor versus dimensionless time for Type-I material pair.

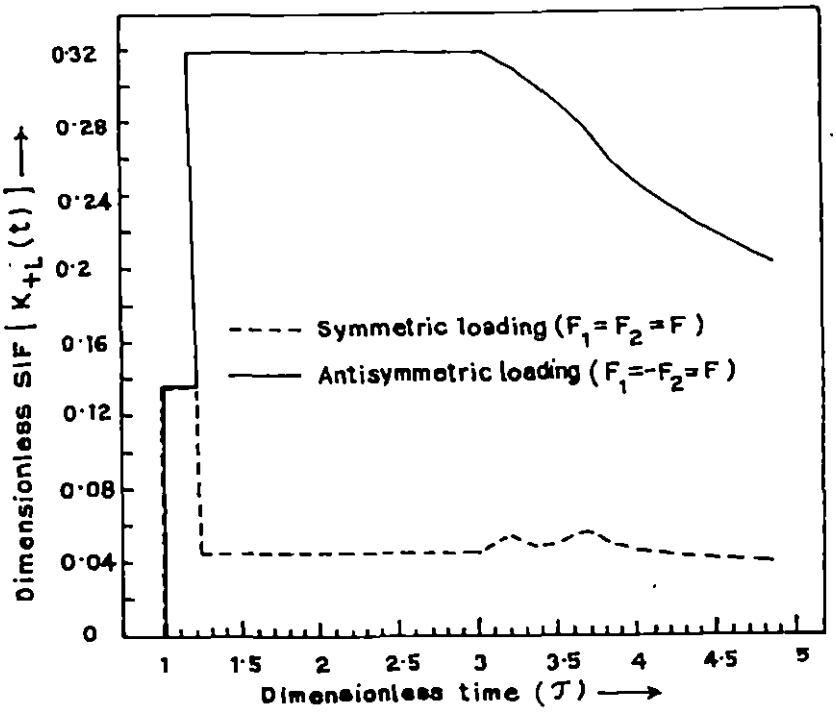

Fig.4. Stress intensity factor versus dimensionless time for Type-II material pair.

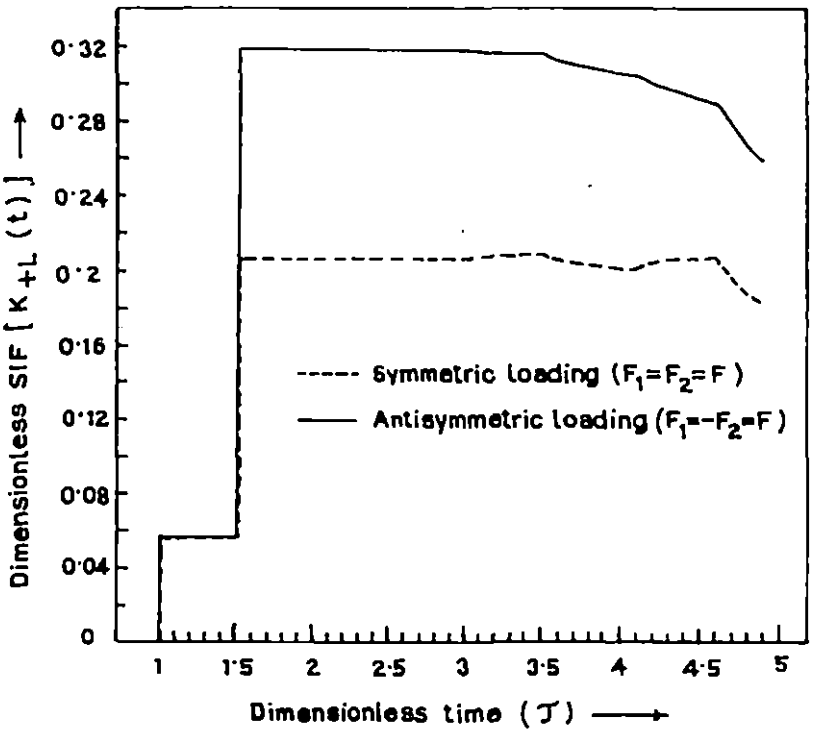

Fig.5. Stress intensity factor versus dimensionless time for Type-III material pair.

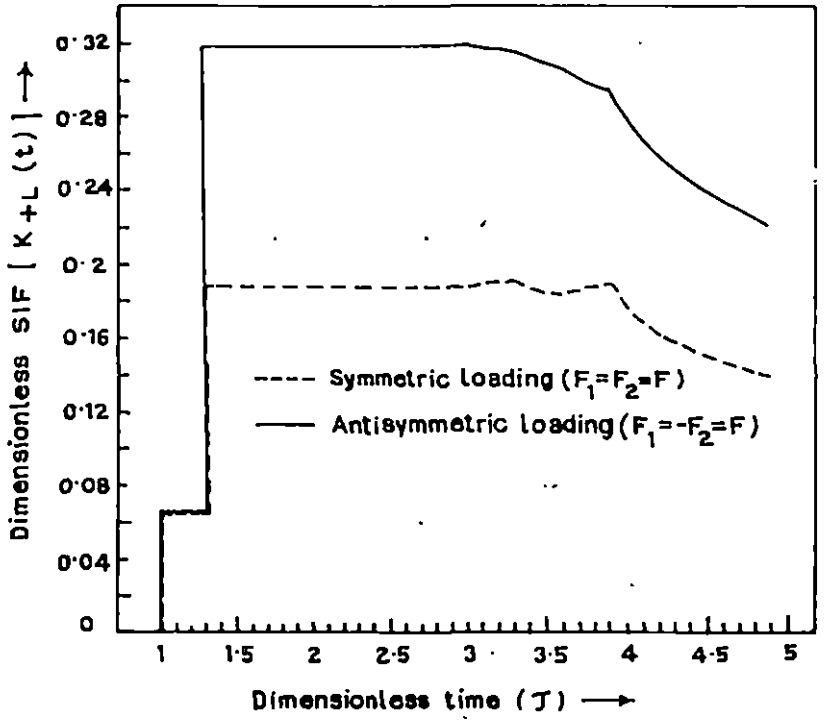

Fig.6. Stress intensity factor versus dimensionless time for Type-IV material pair.

It is interesting to note that after the arrival of the first scattered wave from the opposite edge of the crack, the stress intensity factor gradually decreases in the case of antisymmetric loading.

However in the case of symmetric loading stress intensity factor at first increases when the wave moving from the source along the upper face of the crack surface reaches the crack tip but as soon as the wave from the source moving along the lower face of the crack reaches the crack tip, suddenly it decreases for Type I and Type II material pairs and increases for Type III and Type IV material pairs until the scattered wave from the opposite crack tip arrives when the stress intensity factor shows tendency of increasing but with slow oscillations.

Appendix A

From equation (40) we obtain

$$R^1(\zeta) = \frac{(\mu_1+\mu_2)\sqrt{(\zeta^2+k_2^2)}}{\mu_1\sqrt{(\zeta^2+k_1^2)}+\mu_2\sqrt{(\zeta^2+k_2^2)}} \tag{A.1}$$

$$R^1(\zeta) = R_+^1(\zeta)R_-^1(\zeta) = \frac{1}{\frac{m}{1+m}+\frac{1}{1+m}\sqrt{\frac{\zeta^2+k_1^2}{\zeta^2+k_2^2}}},$$

where

$$m = \frac{\mu_2}{\mu_1}.$$

Taking logarithm on both sides, one obtains

$$\log R^1(\zeta) = \log R_+^1(\zeta) + \log R_-^1(\zeta) = -\log\left[\frac{m}{1+m} + \frac{1}{1+m}\sqrt{\frac{\zeta^2+k_1^2}{\zeta^2+k_2^2}}\right].$$

So

$$\log R_+^1(\zeta) = \frac{1}{2\pi i}\int_{-ic-\infty}^{-ic+\infty}\frac{\log R^1(z)}{z-\zeta}\,dz.$$

Replacing z by -z and using $R^1(-z) = R^1(z)$

$$\log R_+^1(\zeta) = -\frac{1}{2\pi i}\int_{ic-\infty}^{ic+\infty}\frac{\log R^1(z)}{z+\zeta}\,dz = \frac{1}{2\pi i}\int_{ic-\infty}^{ic+\infty}\frac{\log\left[\frac{m}{1+m}\left\{1+\frac{1}{m}\sqrt{\frac{z^2+k_1^2}{z^2+k_2^2}}\right\}\right]}{z+\zeta}\,dz$$

$$= \frac{1}{2\pi i}\int_{ic-\infty}^{ic+\infty}\frac{\log\left[1+\frac{1}{m}\sqrt{\frac{z^2+k_1^2}{z^2+k_2^2}}\right]}{z+\zeta}\,dz$$

$$= \frac{1}{2\pi i}\int_{k_1}^{k_2}\frac{\log\left[1+i\sqrt{\frac{u^2-k_1^2}{m^2(k_2^2-u^2)}}\right]}{u-i\zeta}\,du - \frac{1}{2\pi i}\int_{k_1}^{k_2}\frac{\log\left[1-i\sqrt{\frac{u^2-k_1^2}{m^2(k_2^2-u^2)}}\right]}{u-i\zeta}\,du$$

which yields,

$$R_+^1(\zeta) = \exp\left[\frac{1}{\pi}\int_{k_1}^{k_2}\frac{\tan^{-1}\left[(z^2-k_1^2)/\{m^2(k_2^2-z^2)\}\right]^{1/2}}{(z-i\zeta)}dz\right]. \qquad (A.2)$$

Similarly,

$$R_{-}^{1}(\zeta) = \exp\left[\frac{1}{\pi}\int_{k_1}^{k_2}\frac{\tan^{-1}\left[(z^2-k_1^2)/\{m^2(k_2^2-z^2)\}\right]^{1/2}}{(z+i\zeta)}dz\right]. \quad (A.3)$$

Similarly, it can be shown that

$$R_{\pm}^{2}(\zeta) = \exp\left[-\frac{1}{\pi}\int_{k_1}^{k_2}\frac{\tan^{-1}\left[m^2(k_2^2-z^2)/(z^2-k_1^2)\right]^{1/2}}{(z\mp i\zeta)}dz\right] \quad (A.4)$$

where $R^2(\zeta)$ is given by equation (43).

Using equation (40) or equation (41) it can be shown that

$$K_{\pm}(\zeta) = \left(\frac{\mu_1\mu_2}{\mu_1+\mu_2}\right)^{1/2}(\zeta\pm ik_1)^{1/2}R_{\pm}^{1}(\zeta) \quad (A.5)$$

$$= \left(\frac{\mu_1\mu_2}{\mu_1+\mu_2}\right)^{1/2}(\zeta\pm ik_2)^{1/2}R_{\pm}^{2}(\zeta). \quad (A.6)$$

From either equation (A.5) or equation (A.6) it can be easily shown that

$$K_{-}(-\zeta) = -iK_{+}(\zeta).$$

----x----

[3]INTERACTION OF HORIZONTALLY POLARISED SH-WAVE WITH A GRIFFITH CRACK MOVING ALONG THE BIMATERIAL INTERFACE

1. INTRODUCTION

Scattering of elastic waves by a stationary or moving crack of finite width at the interface of two dissimilar elastic materials is important in view of its application in seismology as well as in fracture mechanics. The diffraction of Love waves by a stationary crack of finite width at the interface was investigated by Neerhoff [1979]. Kuo [1984] carried out analytical and numerical studies of transient response of an interfacial crack between two dissimilar orthotropic half spaces. Srivastava et al [1980] also derived the low frequency solution of the interaction of SH-wave by a Griffith crack at the interface of two bonded dissimilar elastic media.

In the case of cracks of finite size, moving with uniform velocity, loads, for mathematical simplicity, are usually assumed to be independent of time. However, in practice, structures are often required to sustain oscillating loads where the dynamic disturbances propagate through the elastic medium in the form of stress waves. The problem of diffraction of a plane harmonic polarized shear wave by a half-plane crack extended under antiplane strain was first studied by Jahanshahi [1967]. Later Sih and Loeber [1970] and Chen and Sih [1975] also considered the problem of scattering of plane harmonic wave by a running crack of finite length. Recently the high frequency solution of the problem of diffraction of the horizontally polarizes shear wave by a finite crack moving on a bimaterial interface has been investigated by Pal and Ghosh [1993] using Wiener-Hopf technique.

---

[3] **In press, Indian Journal of Pure and Applied Mathematics, 2000.**

In the present paper, we have investigated the low frequency solution of the scattering of plane SH-wave by a finite crack moving on bimaterial interface with uniform velocity. Using moving co-ordinate system and Fourier transform technique, the elastodynamic problem has been reduced to two pairs of dual integral equations. Following Sih and Loeber [1969], the solution is then obtained in terms of a pair of coupled Fredholm integral equations. Finally the singular nature of the stress near about the crack tip has been determined. The numerical values of dynamic stress intensity factor versus demensionless wave number have been depicted by means of graphs for various parameters of material properties, crack speed and the angle of incidence.

2. FORMULATION OF THE PROBLEM AND ITS SOLUTION

Let a plane crack of finite length 2a located at the interface of two bonded dissimilar semi-infinite elastic media be moving with a constant velocity V due to the incidence of plane harmonic SH-wave

$$W_1^{(i)} = W_0 \exp\left[-i\left\{\Lambda_1(X\cos\theta_1 + Y\sin\theta_1) + \Omega T\right\}\right] \tag{2.1}$$

where W_0 is the wave amplitude, Λ_1 wave number, $\Omega(=\Lambda_1 C_1)$ circular frequency, $(\Pi/2 - \theta_1)$ angle of incidence and C_1 is the shear wave velocity in the upper medium denoted by (1).

The crack lies in XZ plane with Z axis directed parallel to the edge of the crack with respect to the rectangular co-ordinate system (X,Y,Z) as shown in Fig.1.

We assume that the displacement and the stress due to scattered fields are

$$W_j = W_j(X,Y)\, e^{-i\Omega T} \tag{2.2}$$

and

$$(\tau_{XZ})_j = \mu_j \frac{\partial W_j}{\partial X} \quad \text{and} \quad (\tau_{YZ})_j = \mu_j \frac{\partial W_j}{\partial Y} \tag{2.3}$$

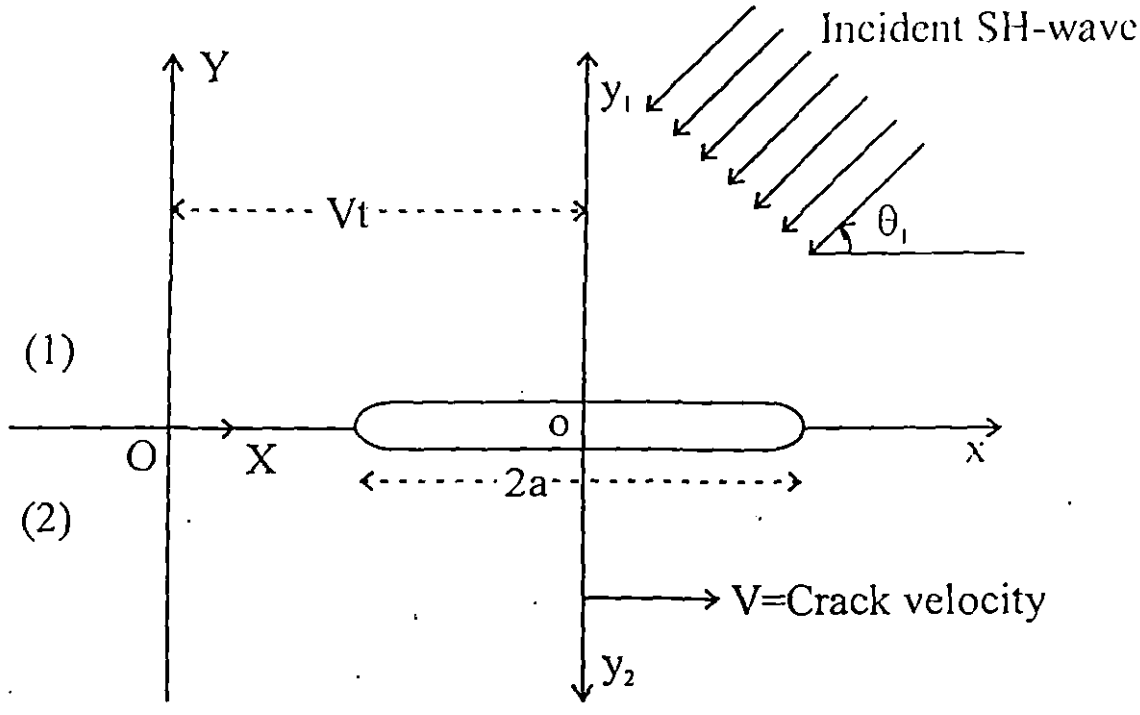

Fig.1. Moving interface crack.

where the subscripts j=1,2 refer to the upper and lower half plane respectively and T denotes time.

The equations of SH wave motion in either elastic half spaces are given by

$$\frac{\partial^2 W_j}{\partial X^2} + \frac{\partial^2 W_j}{\partial Y^2} = \frac{1}{C_j^2}\frac{\partial^2 W_j}{\partial T^2}; \qquad (j=1,2) \tag{2.4}$$

where $C_j = \sqrt{\frac{\mu_j}{\rho_j}}$ is the shear wave velocity and μ_j, ρ_j are co-efficient of rigidity and material density respectively. Without any loss of generality we further assume that $C_1 > C_2$.

Due to the incident wave given in equation (2.1), the reflected and transmitted wave in the absence of the crack may be written as

$$W_1^{(R)} = A\exp\left[-i\left\{\Lambda_1(X\cos\theta_1 - Y\sin\theta_1) + \Omega T\right\}\right]$$

and

$$W_2^{(T)} = B\exp\left[-i\left\{\Lambda_2(X\cos\theta_2 + Y\sin\theta_2) + \Omega T\right\}\right] \tag{2.5}$$

where

$$A = \frac{\mu_1\Lambda_1\sin\theta_1 - \mu_2\Lambda_2\sin\theta_2}{\mu_1\Lambda_1\sin\theta_1 + \mu_2\Lambda_2\sin\theta_2}W_0, \qquad B = \frac{2\mu_1\Lambda_1\sin\theta_1}{\mu_1\Lambda_1\sin\theta_1 + \mu_2\Lambda_2\sin\theta_2}W_0 \tag{2.6}$$

with $\Lambda_1\cos\theta_1 = \Lambda_2\cos\theta_2$.

A, B are the reflected and transmitted wave amplitudes, Λ_j wave number, $\Omega(=\Lambda_j C_j)$ the circular frequency and $(\pi/2 - \theta_1)$ and $(\pi/2 - \theta_2)$ the angles of incidence and refraction respectively.

A set of moving co-ordinate system (x, y_j, z, t) moving along with the crack at a constant velocity V in X-direction is introduced in accordance with

$$x = X - Vt, \quad y_j = s_j Y, \quad z = Z, \quad t = T \tag{2.7}$$

where $s_j^2 = 1 - M_j^2$ and $M_j = V/C_j$ is the Mach number.

$M_j < 1$, since the crack is assumed to travel at subsonic speed.

In terms of moving co-ordinate system (x, y_j, t) equation (2.4) becomes

$$\frac{\partial^2 W_j}{\partial x^2} + \frac{\partial^2 W_j}{\partial y_j^2} + \frac{1}{C_j^2 s_j^2}\frac{\partial}{\partial t}\left[2V\frac{\partial W_j}{\partial x} - \frac{\partial W_j}{\partial t}\right] = 0. \tag{2.8}$$

Further, referred to moving coordinate system, incident and reflected and transmitted wave given by equations (2.1) and (2.5) take the following form,

$$W_1^{(i)} = W_0 e^{-i\omega t}\exp\left[-i\Lambda_1\left(x\cos\theta_1 + \frac{y_1}{s_1}\sin\theta_1\right)\right],$$

$$W_1^{(R)} = A e^{-i\omega t}\exp\left[-i\Lambda_1\left(x\cos\theta_1 - \frac{y_1}{s_1}\sin\theta_1\right)\right]$$

and $$W_2^{(T)} = B e^{-i\omega t}\exp\left[-i\Lambda_2\left(x\cos\theta_2 + \frac{y_2}{s_2}\sin\theta_2\right)\right] \tag{2.9}$$

where $\omega = \Omega\,\alpha$ and $\alpha = (1 + M_1\cos\theta_1) = (1 + M_2\cos\theta_2)$ (2.10)

It is convenient to write the solution of the equation (2.8) in the form

$$W_j(x,y_j,t) = W_j(x,y_j)\,e^{-i\omega t} = w_j(x,y_j)\exp[\,i(\lambda_j M_j x - \omega t)\,] \tag{2.11}$$

where $\lambda_j = \frac{\Lambda_j}{s_j^2}\alpha$. (2.12)

Substitution of equation (2.11) into equation (2.8) yields the Helmhlotz equation governing w_j

$$\frac{\partial^2 w_j}{\partial x^2} + \frac{\partial^2 w_j}{\partial y_j^2} + \lambda_j^2 w_j = 0. \tag{2.13}$$

The solution of equation (2.13) can be written as

$$w_j(x,y_j) = \frac{1}{2\pi}\int_{-\infty}^{\infty} A_j(\xi)\,e^{-i\xi x - \beta_j|y_j|}\,d\xi \tag{2.14}$$

where $\beta_j = \sqrt{\xi^2 - \lambda_j^2}$. (2.15)

From equations (2.11) and (2.14) the displacement components of the diffracted field can be expressed as

$$W_j(x,y_j) = \frac{1}{2\pi}\int_{-\infty}^{\infty} B_j(\xi)\,e^{-i\xi x - \gamma_j|y_j|}\,d\xi \tag{2.16}$$

where

$$\gamma_j = \sqrt{(\xi + \lambda_j M_j)^2 - \lambda_j^2}, \qquad B_j(\xi) = A_j(\xi + \lambda_j M_j) \tag{2.17}$$

The unknown quantities $B_1(\xi)$ and $B(\xi)$ are to be determined from the following boundary conditions

$$\mu_1 s_1 \frac{\partial W_1}{\partial y_1} = \mu_2 s_2 \frac{\partial W_2}{\partial y_2} \quad \text{for all } x,\ y_j = 0$$

$$W_1 = W_2; \qquad |x| > a; \qquad Y_j = 0$$

$$\frac{\partial W_1}{\partial y_1} + \frac{\partial W_1^{(i)}}{\partial y_1} + \frac{\partial W_1^{(R)}}{\partial y_1} = 0; \quad |x| < a; \quad y_j = 0. \tag{2.18}$$

From the first boundary condition of equations (2.18) one obtains

$$\mu_1 s_1 \gamma_1 B_1(\xi) + \mu_2 s_2 \gamma_2 B_2(\xi) = 0. \tag{2.19}$$

The other two boundary conditions yield the following dual integral equations

$$\frac{1}{2\pi} \int_{-\infty}^{\infty} P_1(\xi) e^{-i\xi x} d\xi = 0; \quad |x| > a, \quad y_j = 0$$

and

$$\frac{1}{2\pi} \int_{-\infty}^{\infty} E_1(\xi) P_1(\xi) e^{-i\xi x} d\xi = -D_1 e^{-i\Lambda_1 x \cos\theta_1}; \quad |x| < a \tag{2.20}$$

where

$$P_1(\xi) = \frac{s_1 \mu_1 \gamma_1 + s_2 \mu_2 \gamma_2}{\gamma_2} B_1(\xi) \tag{2.21}$$

$$E_1(\xi) = \frac{\gamma_1 \gamma_2}{s_1 \mu_1 \gamma_1 + s_2 \mu_2 \gamma_2} \tag{2.22}$$

$$D_1 = \left(\frac{2\mu_2 \Lambda_2 \sin\theta_2}{\mu_1 \Lambda_1 \sin\theta_1 + \mu_2 \Lambda_2 \sin\theta_2} \right) \frac{i\Lambda_1 \sin\theta_1}{s_1} W_0 \tag{2.23}$$

The equation (2.20) can further be reduced to two sets of dual integral equations. They are

$$\frac{2}{\pi} \int_0^{\infty} P_{1e}(\xi) \cos(\xi x) d\xi = 0; \quad |x| > a, \quad y_j = 0;$$

$$\frac{2}{\pi} \int_0^{\infty} E_{1e}(\xi) P_{1e}(\xi) \cos(\xi x) d\xi$$

$$= -2D_1\cos(\Lambda_1 x\cos\theta_1) - \frac{2}{\pi}\int_0^\infty E_{1o}(\xi)P_{1o}(\xi)\cos(\xi x)\,d\xi; \quad |x|<a. \qquad (2.24)$$

and $$\frac{2}{\pi}\int_0^\infty P_{1o}(\xi)\sin(\xi x)\,d\xi = 0; \quad |x|>a, \quad y_j = 0;$$

$$\frac{2}{\pi}\int_0^\infty E_{1e}(\xi)P_{1o}(\xi)\sin(\xi x)\,d\xi$$

$$= -2D_1\sin(\Lambda_1 x\cos\theta_1) - \frac{2}{\pi}\int_0^\infty E_{1o}(\xi)P_{1e}(\xi)\sin(\xi x)\,d\xi; \quad |x|<a. \qquad (2.25)$$

where

$$P_1(\xi) = \frac{1}{2}\left[P_1(\xi)+P_1(-\xi)\right] + \frac{1}{2}\left[P_1(\xi)-P_1(-\xi)\right] = P_{1e}(\xi) + P_{1o}(\xi)$$

$$E_1(\xi) = \frac{1}{2}\left[E_1(\xi)+E_1(-\xi)\right] + \frac{1}{2}\left[E_1(\xi)-E_1(-\xi)\right] = E_{1e}(\xi) + E_{1o}(\xi). \qquad (2.26)$$

The problems in equation (2.24) and (2.25) are respectively even and odd in x. The solution procedure described in Sih and Loeber [1969], can be used to solve equations (2.24) and (2.25) and the result is a coupled Fredholm integral equation of the second kind. In order to solve equations (2.24) and (2.25) it is assumed that

$$P_{1e}(\xi) = \frac{\pi D_1 a^2}{K}\int_0^1 \sqrt{s}\,\Delta_1(s)\,J_0(a\xi s)\,ds \qquad (2.27)$$

$$P_{1o}(\xi) = \frac{\pi D_1 a}{K\xi}\left[\int_0^1 \sqrt{s}\,\Gamma_1(s)\,J_0(a\xi s)\,ds - i\Omega_1(1)J_0(a\xi)\right] \qquad (2.28)$$

where $$i\Omega_1(1) = \int_0^1 \sqrt{s}\,\Gamma_1(s)\,ds \qquad (2.29)$$

Substitution of equations (2.27) and (2.28) in equations (2.24) and (2.25) yields the following coupled integral equations for the determination of $\Delta_1(s)$ and $\Gamma_1(s)$

$$\Delta_1(s) - \int_0^1 \Delta_1(\eta)M_1(s,\eta)\,d\eta - \int_0^1 \Gamma_1(\eta)\left[N_1(s,\eta) - \sqrt{\eta}N_1(s,1)\right]d\eta$$

$$= \sqrt{s}J_0(\Lambda_1 as\cos\theta_1);$$

$$\Gamma_1(s) - \int_0^1 \Delta_1(\eta)\left\{L_1(s,\eta) - \frac{K'a}{K}M_1(s,\eta)\right\}d\eta +$$

$$+ \int_0^1 \Gamma_1(\eta)\left\{\frac{K'a}{K}\left[N_1(s,\eta) - \sqrt{\eta}N_1(s,1)\right] - \left[M_1(s,\eta) - \sqrt{\eta}M_1(s,1)\right]\right\}d\eta$$

$$= \sqrt{s}\left(\Lambda_1 a\cos\theta_1 - \frac{K'a}{K}\right) J_0(\Lambda_1 as\cos\theta_1); \qquad (2.30)$$

where $$K = -\frac{1}{(s_1\mu_1 + s_2\mu_2)} \qquad (2.31)$$

$$K' = -\frac{(\lambda_1 M_1 s_2\mu_2 + \lambda_2 M_2 s_1\mu_1)}{(s_1\mu_1 + s_2\mu_2)^2} \qquad (2.32)$$

$$M_1(s,\eta) = \frac{\sqrt{s\eta}}{K}\int_0^\infty \xi H_{1e}(\xi/a)J_0(\xi\eta)J_0(\xi s)d\xi \qquad (2.33)$$

$$N_1(s,\eta) = \frac{\sqrt{s\eta}}{K}\int_0^\infty \frac{a}{\xi}E_{1o}(\xi/a)J_0(\xi\eta)J_0(\xi s)d\xi \qquad (2.34)$$

$$L_1(s,\eta) = \frac{\sqrt{s\eta}}{K}\int_0^\infty a\xi H_{1o}(\xi/a)J_0(\xi\eta)J_0(\xi s)d\xi \qquad (2.35)$$

in which $H_{1e}(\xi)$ and $H_{1o}(\xi)$ are defined as

$$H_{1e}(\xi) = \frac{E_{1e}(\xi)}{\xi} + K \to O(\xi^{-2}) \quad \text{as } \xi \to \infty$$

$$H_{1o}(\xi) = E_{1o}(\xi) + K' \to O(\xi^{-2}) \quad \text{as } \xi \to \infty. \qquad (2.36)$$

3. STRESS INTENSITY FACTOR

Since the condition of the crack propagation is controlled by the stresses near the crack tips, we are mainly interested in determining the singular behaviour of the stress field near the crack tips.

With the aid of equation (2.16) and (2.21) the stress in medium 1 can be written as

$$\left(\tau_{yz}\right)_1 = \mu_1 s_1 \frac{\partial W_1}{\partial y_1} = -\frac{\mu_1 s_1}{2\pi}\int_{-\infty}^{\infty} E_1(\xi) P_1(\xi) e^{-i\xi x - \gamma_1 y_1}\, d\xi. \qquad (3.1)$$

For an examination of the singular behaviour of the stress near the crack tip (x=±a) it is sufficient to consider the domonating terms in the integrand of the integral (3.1) as $|\xi| \to \infty$.

Accordingly near the crack tip

$$\left[\left(\tau_{yz}\right)_1\right]_{\text{at crack tip}} = -\frac{s_1 \mu_1}{\pi(s_1\mu_1 + s_2\mu_2)} \times$$

$$\times \left[\int_0^{\infty} \xi e^{-\xi y_1} P_{1e} \cos(\xi x)\, d\xi - i\int_0^{\infty} \xi e^{-\xi y_1} P_{1o} \sin(\xi x)\, d\xi\right]. \qquad (3.2)$$

Further as $|x| \to \infty$

$$P_{1e}(\xi) = \frac{\pi D_1 a}{K\xi}\Delta_1(1) J_1(a\xi) + \ldots\ldots$$

$$P_{1o}(\xi) = -\frac{i\pi D_1 a}{K\xi}\Omega_1(1) J_0(a\xi) + \ldots\ldots \qquad (3.3)$$

Substituting the asymptotic expression of $P_{1e}(\xi)$ and $P_{1o}(\xi)$ as given by equation (3.3) in equation (3.2) the singular stress field around x=a, y=0 is obtained as

$$\left[\left(\tau_{yz}\right)_1\right]_{x=a,y=0} = -\frac{\mu_1 s_1 D_1\sqrt{a}}{\sqrt{2r}}\left\{\Omega_1(1) + \Delta_1(1)\right\} f(s_1) + O(1)$$

$$= \frac{\sigma_1\sqrt{a}}{\sqrt{2r}}\left[\frac{\mu_1 \sin\theta_2}{\mu_1 + \mu_2 \cot\theta_1 \tan\theta_2}\left(\Omega_1(1) + \Delta_1(1)\right)\right] f(s_1) + O(1) \qquad (3.4)$$

where

$$f^2(s_1) = \frac{\sec\phi}{2}\left[\left(1 + s_1^2\tan^2\phi\right)^{-1/2} + \left(1 + s_1^2\tan^2\phi\right)^{-1}\right] \qquad (3.5)$$

$$r = \sqrt{(x-a)^2 + y^2}, \qquad \phi = \tan^{-1}\left(\frac{y}{x-a}\right) \qquad (3.6)$$

and $\sigma_1 = -2\, i\, \mu_2\, A_2\, W_0.$ (3.7)

Dynamic stress intensity factor K_1 is defined by

$$K_1 = \sigma_1\sqrt{a}\left[\frac{\mu_1 \sin\theta_2}{\mu_1 + \mu_2 \cot\theta_1 \tan\theta_2}\left(\Omega_1(1) + \Delta_1(1)\right)\right] \qquad (3.8)$$

While studying the dynamic crack propagation the determination of stress intensity factor is important because it supplies useful information regarding the rate at which elastic and kinetic energies are released by the propagating crack.

4. NUMERICAL RESULTS AND DISCUSSIONS

Numerical results have been calculated to plot normalized stress intensity factor $|K_1/(\sigma_1\sqrt{a})|$ at the carck tip x=a, y=0 versus the normalized wave number $\Lambda_1 a$ for different values of the Mach number M_1 and the angle of incidence for the following sets of materials :

First set :

Steel : $\rho_1 = 7.6$ gm/cm^3, $\mu_1 = 8.32 \times 10^{11}$ dyne/cm^2

Aluminium : $\rho_2 = 2.7$ gm/cm^3, $\mu_2 = 2.63 \times 10^{11}$ dyne/cm^2

Second set :

Wrought iron : $\rho_1 = 7.8$ gm/cm^3, $\mu_1 = 7.7 \times 10^{11}$ dyne/cm^2

Copper : $\rho_2 = 8.96$ gm/cm^3, $\mu_2 = 4.5 \times 10^{11}$ dyne/cm^2

The numerical results have been obtained for low frequencies. The case $M_1=0$ corresponds to the stationary crack solution. It is found that by increasing the crack speed, the dimensionless stress intensity factor $|K_1/(\sigma_1\sqrt{a})|$ decreases with the normalized wave number $\Lambda_1 a$. It is interesting to note that as the velocity of the crack increases, the picks of the curves decreases in magnitude and occur at lower values of $\Lambda_1 a$ (Figs. 2 - 7). For both the pair of solids, graphs of stress intensity factor versus normalised wave number ($\Lambda_1 a$) have been plotted for the angles $\theta_1=\pi/3$, $\theta_1=\pi/4$, and as well as $\theta_1=\pi/6$. It is also found that for a given pair of materials and for a given Mach number, the peak values of the stress intensity factors decrease with the decrease in the values of θ_1.

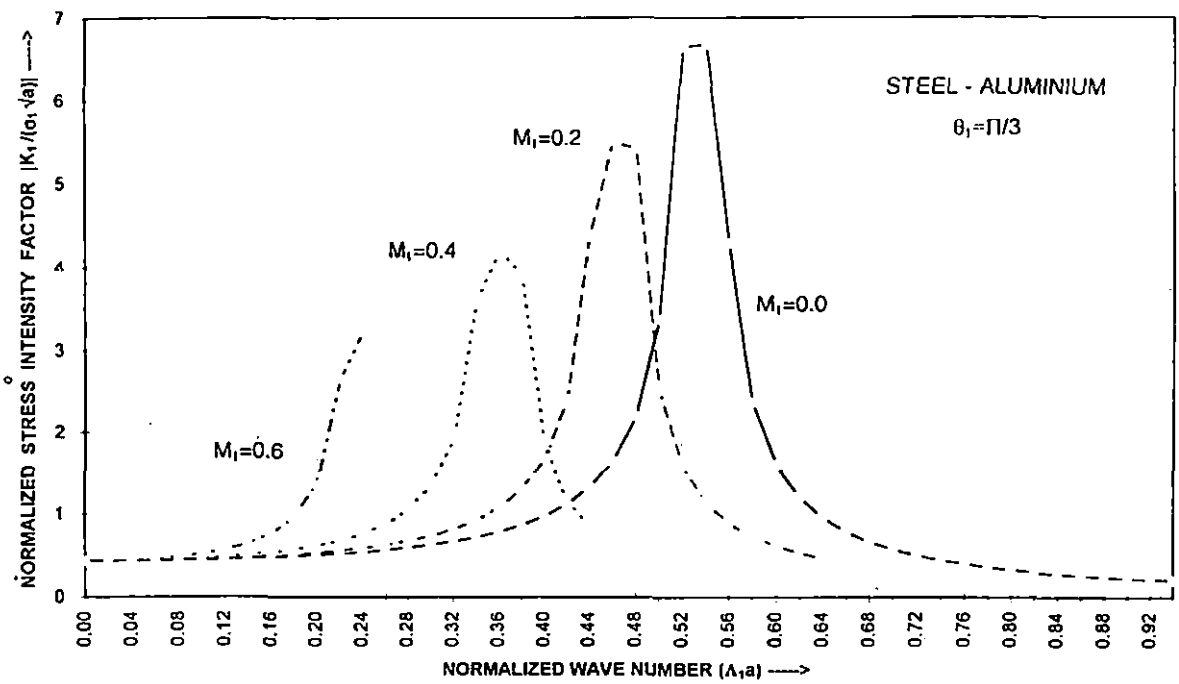

Fig.2 Stress intensity factor vs wave number.

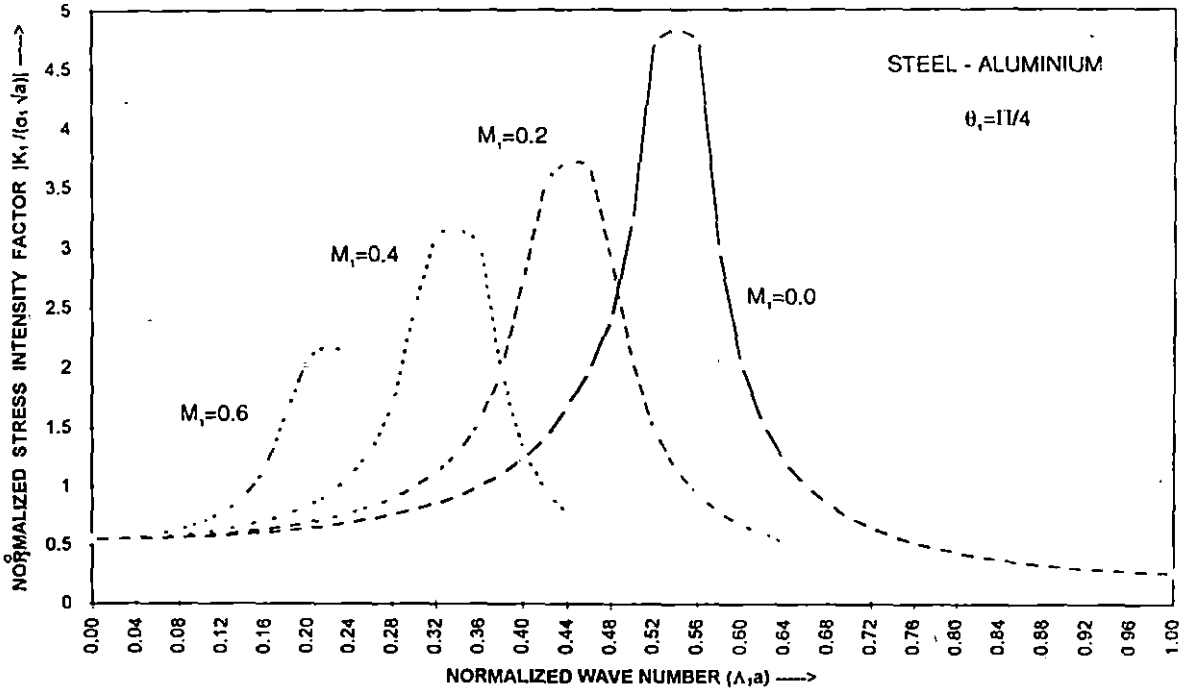

Fig.3 Stress intensity factor vs wave number.

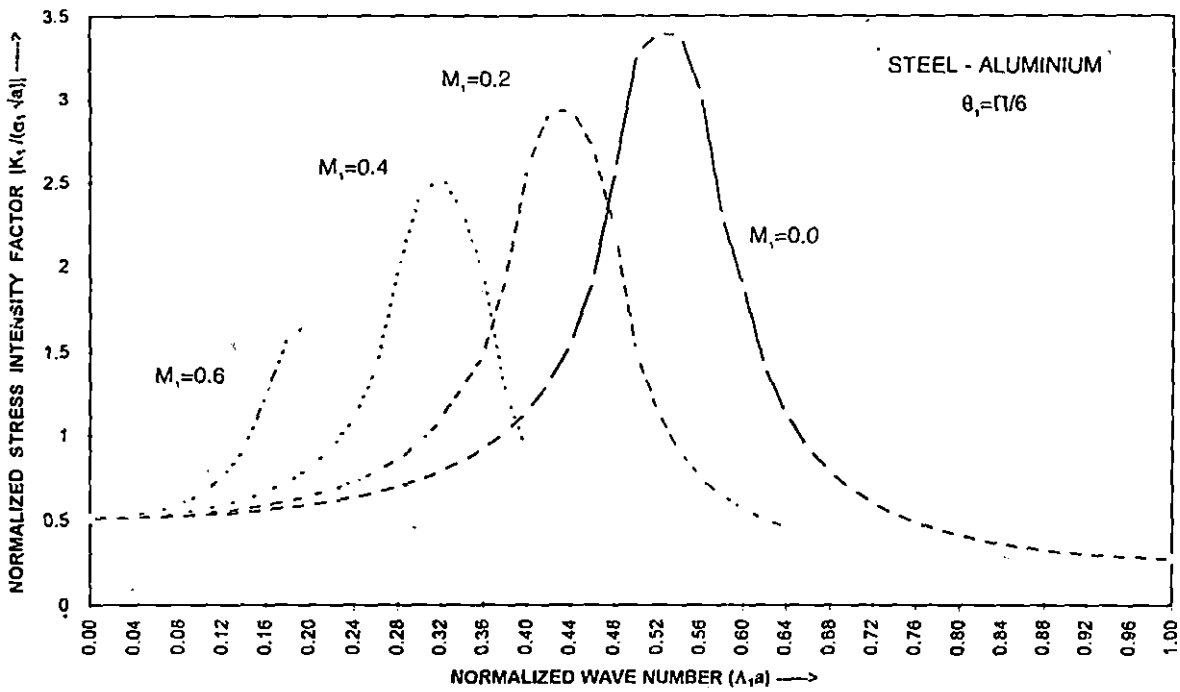

Fig.4 Stress intensity factor vs wave number.

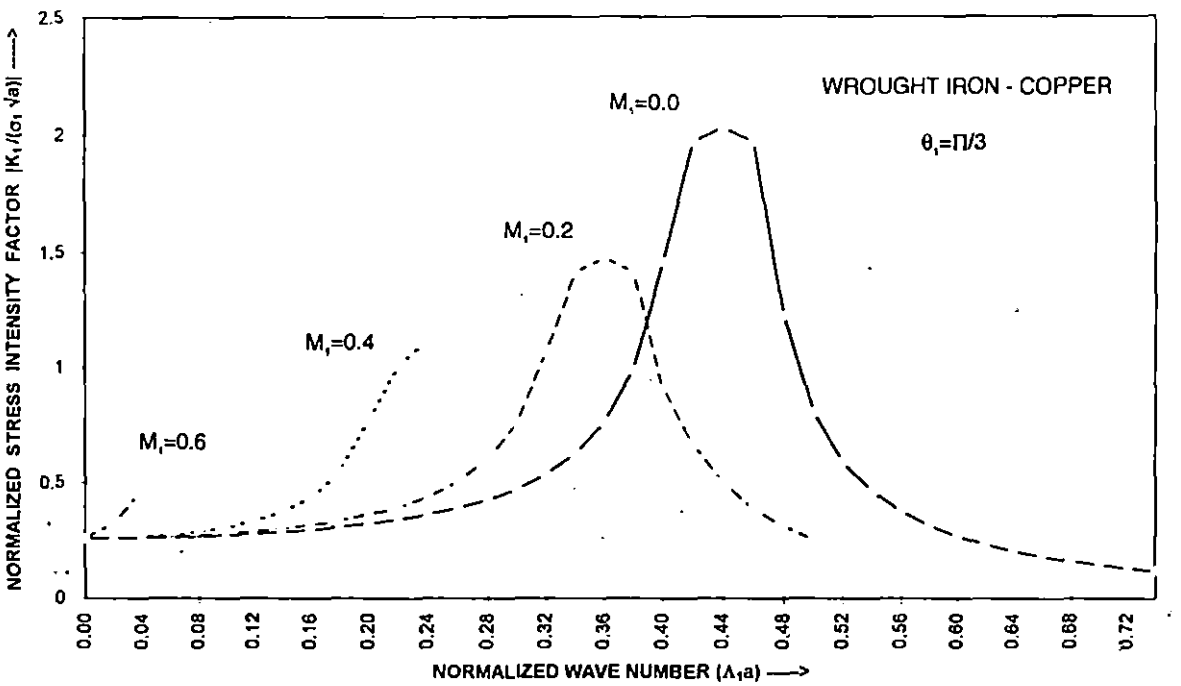

Fig.5 Stress intensity factor vs wave number.

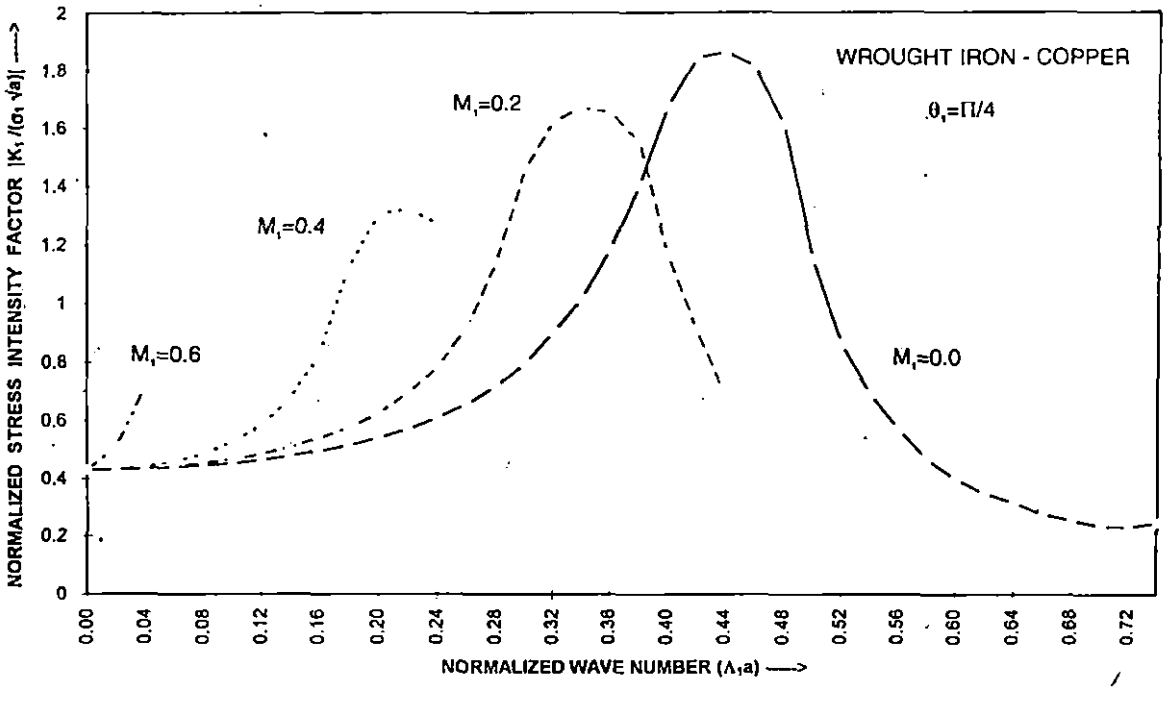

Fig.6 Stress intensity factor vs wave number.

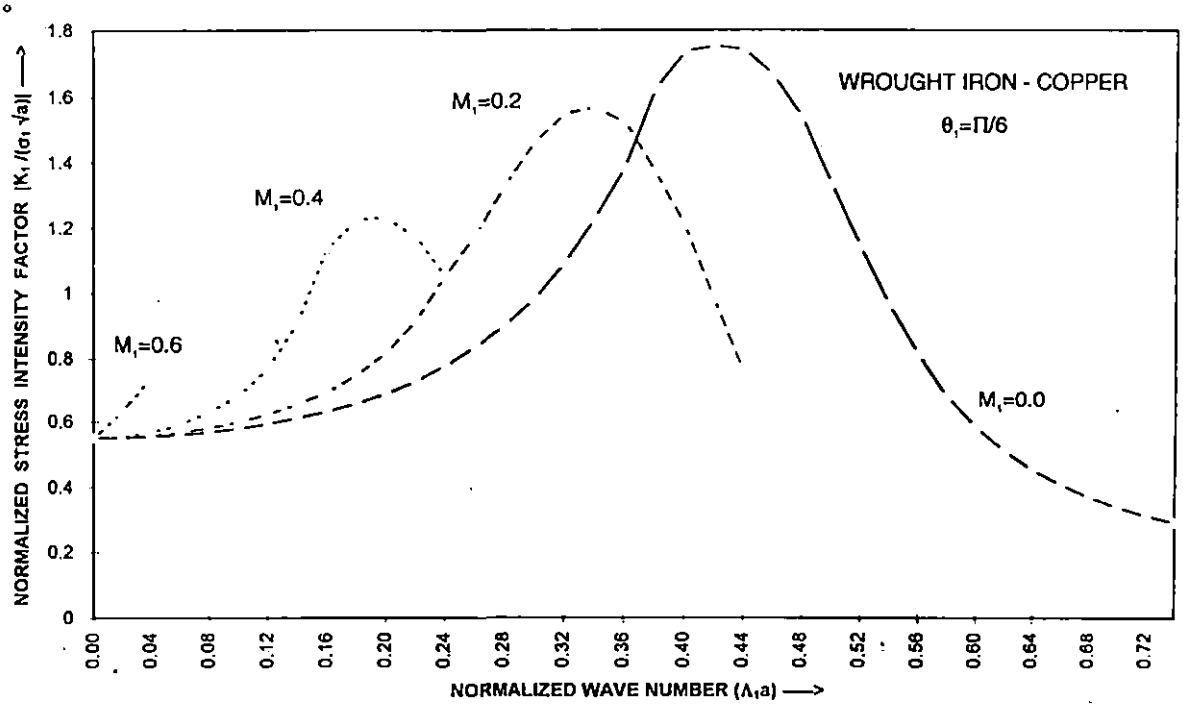

Fig.7 Stress intensity factor vs wave number.